I give permission for public access to my thesis and for copying to be done at the discretion of the archives' librarian and/or the College library.

_____ _____

Signature Date

MOTORS AND MITOSIS: CHARACTERIZING THE ROLE OF DYNEIN IN MAMMALIAN EPITHELIAL SPINDLE POSITIONING PHENOMENA

by

Kaitlin Brooke

A Paper Presented to the

Faculty of Mount Holyoke College in

Partial Fulfillment of the Requirements for

the Degree of Bachelors of Arts with

Honor

Department of Biological Sciences

South Hadley, MA 01075

May 2010

This paper was prepared

under the direction of

Professor Rachel Fink

for eight credits.

ACKNOWLEDGMENTS

It is difficult to express the depth of my gratitude to all of the people who supported this thesis work. I am particularly indebted to my advisor Pat Wadsworth, who encouraged me to expand my summer research in her lab into an honors thesis. Without your incredible generosity and your willingness to share your vast knowledge of cell division with me, this thesis would not exist. I wish to thank everyone in the Wadsworth lab that has helped me over the course of my research, especially Alyssa Gable, Liz Collins, Carey Fagerstrom, Janel Pariseau, Nick Ferenz, Nan Ma, and Jessica Faraci.

I am incredibly thankful for the wisdom of my advisor at Mount Holyoke, Rachel Fink. Your reassurance, invaluable guidance, and your patience while reading through many drafts of this thesis cannot be understated. I wish to thank the Biology Department of Mount Holyoke College for funding and support.

I would like to thank my friends who sustained me throughout this process, and my sister Margaret for putting up with me. Finally, I wish to express my perpetual gratefulness to my parents Marvin and Kathleen for introducing me to the word of science – this thesis is dedicated to you.

TABLE OF CONTENTS

LIST OF FIGURES

ABSTRACT

Reproduction distinguishes living organisms from inanimate objects, as cells cannot be made except by division from preexisting cells. Despite the importance of proper cell division for growth, aging, healing, and the prevention of diseases such as cancer, many of the complicated protein interactions involved remain a mystery. Mitosis, the segregation of replicated chromosomes to two new daughter cells, is central to the process of cell division. The forces generated by motor proteins, a special class of proteins able to convert chemical energy from ATP into mechanical energy, are necessary for the movements of the cytoskeleton during mitosis.

Dynein is a motor protein that walks along the microtubules of the mitotic spindle, performing several essential roles throughout the phases of mitosis. Research in budding yeast and other model systems has implicated dynein located at the cell cortex as a key player in spindle positioning (Kozlowski et al., 2007; Carminati and Stearns, 1997). The regulation and mechanics of spindle positioning are poorly understood yet critical for both asymmetric and symmetric cell divisions.

The characterization of spindle positioning phenomena in a line of mammalian epithelial cells revealed a pattern of asymmetric spindle position at anaphase onset followed by unequal movement of each set of sister chromatids in a significant subpopulation of cells. In addition to phase contrast observation of spindle positioning, microscopic observation of mammalian epithelial cells expressing fluorescent gamma tubulin revealed asymmetric movement of each spindle pole during anaphase. Immunofluorescent fixing and staining of mammalian epithelial cells suggested that dynein localized to the cell cortex plays a role in spindle positioning phenomena.

INTRODUCTION

Cell Division: Motors and Mitosis

The fundamental ability to reproduce is common to all organisms. Life forms as disparate as the lithotrophic bacteria *Thermus aquaticus*, vertebrate optic nerve cells, the fission yeast *S. pombe*, and the xylem parenchyma cells in a 1,000 year old sequoia all make new cells by division from preexisting ones. Reproduction is one of the basic processes that distinguish living organisms from inanimate objects. In vertebrates such as humans, fertilized eggs grow into embryos through a series of mitotic cell divisions, and continue to develop into a fully formed adult as their cells differentiate and divide further. The eggs and sperm necessary for sexual reproduction come from a special type of cell division called meiosis, in which one cell divides into four new haploid cells, forming gametes. In addition to the essential role cell division plays in the creation and development of a new organism, cells must divide throughout the lifetime of a multicellular organism to replace injured or dead cells. The 10^{14} cells that make up the human body will divide approximately 10^{16} times during the human lifespan (Cairns, 1975; Evan and Vousden, 2001). Despite the importance of cell division for growth, aging, healing, and the progression of diseases such as cancer, many of the biochemical and molecular interactions involved remain a mystery.

In eukaryotes, the process of cell division consists of DNA replication, growth, mitosis and cytokinesis. In mitosis, the sister chromosomes are segregated, splitting the two copies of the genome equally in advance of cytokinesis, at which point the organelles and cytosol are partitioned. The cytoskeleton of the cell organizes and transports chromosomes by forming a microtubule based structure called the spindle. Microtubules are made up of α– and β– tubulin dimers organized as protofilaments into hollow tube, and provide structure in cells while undergoing dynamic growth and catastrophe from the plus end (Alberts, 2008). Microtubules are not solely structural elements; they can also generate force within the cell in three ways. Microtubule growth can push on an object such as the cell membrane, shrinking microtubules can pull on objects attached to the microtubule, and motor proteins can transmit force through microtubules (Tolic-Norrelykke, 2010). The motor proteins that walk along microtubules exert force by undergoing conformational changes powered by hydrolysis of ATP in the motor domain (Alberts, 2008). Motor proteins can carry "cargoes" of organelles, such as mitochondria, or other cytoskeletal structures, depending on the tail domain of the motor (Alberts, 2008). The highly regulated phases of mitosis are distinguished by rearrangements of both the cytoskeleton and the genetic material, mediated by motor proteins.

The onset of mitosis, prophase, is characterized by the visible condensation of nuclear DNA as seen under a light microscope (Figure 1a). The images of mammalian epithelial cells expressing fluorescent tubulin to visualize

microtubules reveal the mitotic spindle (see Figure 2a), which begins to form between the duplicated centrosomes outside the nucleus during prophase (Alberts, 2008). The breakdown of the nuclear envelope indicates the transition to prometaphase (Figure 1a), the point at which microtubules from the spindle begin to attach to the kinetochores of the condensed sister chromosomes (Alberts, 2008). The process of arranging microtubules and chromosomes in metaphase (Figure 2b, Figure 1b) will last until each pair of sister chromosomes is lined up on the metaphase plate (Alberts, 2008). The metaphase spindle in Figure 2b clearly shows interpolar and kinetochore microtubules between the spindle poles as well as astral microtubules reaching towards the cell cortex.

The cell cannot proceed through mitosis without all of the components of the spindle in exactly their proper place; the metaphase to anaphase transition provides one of the checkpoints to prevent loss of a chromosome or other catastrophic errors of cell division (Alberts, 2008). Anaphase (Figure 2c) is divided into two different stages of spindle elongation. During anaphase A (Figure 1c), the kinetochore microtubules shorten by depolymerization in order to separate the sister chromosomes into two sets of daughter chromosomes, each set carrying an entire replicated genome. During anaphase B (Figure 1d) the spindle poles move apart to further segregate the daughter chromosomes. Chromosome separation is followed by decondensation of the chromosomes during telophase, reformation of the nuclear envelope around each new genome, and formation of the contractile ring (Alberts, 2008). The contractile ring, a structure of actin

filaments and proteins, constricts to form the cleavage furrow and divide the cytoplasm and organelles to create two new complete daughter cells, a process called cytokinesis (Alberts, 2008). The entire process of mitosis, from prophase to cytokinesis, can take anywhere from 30 minutes to an hour and a half in mammalian cells, depending upon the type of cell (Altman and Katz, 1962).

At every step of mitosis, the microtubules and actin filaments that make up the cytoskeleton indicative of Eukaryotes undergo dynamic and highly regulated movement. The incredibly complex phenomenon of cell division, in which every element necessary for life is duplicated and partitioned into two new living cells, relies on motor proteins to exert force by converting chemical energy to mechanical energy and in effect walking along microtubules. There are two main classes of motor proteins associated with microtubules, the generally plus-end directed kinesin family and the minus-end directed motor protein dynein.

Dynein Structure and Function

The dynein family of minus-end directed motor proteins includes two types of dynein, axonemal dynein and cytoplasmic dynein. Although axonemal dynein was the type first discovered in the cilia of the protozoan *Tetrahymena* in 1965, cytoplasmic dynein has since been found to have more roles in the cell, including many required for the completion of mitosis (Gibbons and Rowe, 1965). Cytoplasmic dynein (see Figure 3) performs several dynamic processes both in interphase and during cell division, all of which depend on complex

interactions with other molecules. Because of the intricate temporal-spatial relationships between a myriad of proteins during mitosis, fundamental information about the regulation, structure and function of dynein remains to be elucidated.

The relatively large size of the dynein motor protein complex, over 1.2 MDa, has complicated experimental protocols and delayed research on the motor protein compared to its better known cousins, myosin and kinesin (Oiwa and Sakakibara, 2005; Gennerich and Vale, 2009). Cytoplasmic dynein is generally thought to exist as a homodimer of two heavy chains, each of which is greater than 500KDa (Oiwa and Sakakibara, 2005). It has been proposed that dynein may also exist as monomers or trimers that perform different functions within the cell (King, 2000). The elaborate structure of the functional dynein complex also includes several associated subunits and colocalizing proteins, in addition to the cytoplasmic heavy chain 1 that makes up the dynein homodimer (Myers et al., 2007; Gennerich and Vale, 2009).

The functional domains of motor proteins are generally organized into the motor domain, which includes an ATPase enzyme to catalyze the dephosphorylation of ATP, and the tail domain. The head, stalk and linker regions of the dynein motor domain are found at the C-terminal end of the 520 KDa heavy chain (Figure 3 and 4; Gennerich and Vale, 2009). The C-terminal motor domain includes the microtubule binding and ATPase regions, while the N-terminal tail domain binds dynein to its cargo, which could be other microtubules,

vesicles or other proteins (Mizuno et al., 2007). The coiled-coil stalk of the motor domain is hypothesized to transmit information between the ATP binding region and the microtubule binding region of the heavy chain, which are separated by a relatively large distance compared to kinesin or myosin (Oiwa and Sakakibara, 2005). The protein sequence of cytoplasmic mouse dynein heavy chain, hereafter referred to as dynein, has been determined (Figure 4). Although a crystal structure for dynein has yet to be resolved, a working model of the protein is diagrammed by Gennerich and Vale, showing the consensus protein structure of cytoplasmic mouse dynein heavy chain in Figure 3 (Gennerich and Vale, 2009).

The dynein complex includes multiple subunits of intermediate chains, light intermediate chains and light chains including Tctex1, Roadblock and LC8 (Figure 3) (Myers et al., 2007; Gennerich and Vale, 2009). Many of these subunits bind colocalizing regulatory proteins, and their various localizing and regulatory functions remain open avenues of research. The localization of dynein or dynein subunits in live cells could provide information about the molecular interactions of dynein within the cell. The intermediate chain forms a scaffold by binding directly to the heavy chain and three light chains, as well as binding to the $p150^{Glued}$ subunit of dynactin to mediate dynein-dynactin interaction (Myers et al., 2007). Dynactin is a large multisubunit regulator of dynein that is required for the majority of its functions and generally colocalizes with dynein, making it an excellent probe for dynein (Karki and Holzbaur, 1999; Gaetz and Kapoor, 2004). Dynein interacts with several other proteins essential to mitosis, from regulatory

proteins to other motors. For example, the nuclear mitotic apparatus (NuMA) protein works with dynein to organize microtubules at the spindle and cell cortex. The role of these complex interactions in dynein localization, as well as the role of posttranslational modifications such as phosphorylation of the intermediate chain and other associated subunits, have yet to be fully clarified (Vaughan et al., 2001).

Dynein plays many roles in an interphase cell, including positioning of the Golgi complex and the transportation of organelles such as lysosomes and nuclei along the microtubule cytoskeleton. The function of dynein during mitosis is even more varied and complicated, as it depends on location and phase of mitosis as well as various regulatory proteins, in particular dynactin (Vaughan et al., 2001; Markus et al., 2009). Some of the mitotic processes for which dynein is required include assembling the spindle, aiding in nuclear envelope breakdown, capturing and organizing the chromosomes, focusing the spindle poles and segregating the chromosomes (Pfarr et al., 1990; Gennerich and Vale, 2009; Markus et al., 2009). Because of the early and essential function of dynein in spindle assembly, later processes involving dynein, such as spindle positioning, have been experimentally difficult to investigate (Pecreaux et al., 2006). Given the many diverse processes mediated by dynein, we have much to learn about what directs dynein to different parts of the cell at the proper time during mitosis, and what functions it performs in each location.

One key responsibility of dynein during mitosis is to adjust the length and position of the spindle. Dynein works to oppose the plus end directed kinesin Eg5 in an antagonistic relationship that to determines spindle length by sliding interpolar microtubules into position (Chakravarty et al., 2004; Tanenbaum et al., 2008). The regulatory role of dynein during mitosis has been demonstrated by inhibition experiments in mitotic *Xenopus* extracts, commonly used as a tool for in vitro investigation of mitosis. The coiled-coil 1 (CC1) fragment of $p150^{Glued}$ is a recombinant protein that binds to dynein and inhibits dynactin (Karki and Holzbaur, 1999). Inhibition of dynein by CCI microinjection in *Xenopus* extract results in an elongated spindle phenotype, demonstrating the importance of dynein in adjusting spindle length during both prometaphase and metaphase (Gaetz and Kapoor, 2004). Studies such as these must be combined with detailed localization and other *in vivo* assays to elucidate dynein-dependent processes that remain poorly understood. One subject of inquiry concerns the mechanism by which dynein acts as a force generator at the cortex of the cell, since cortical forces have been implicated in spindle positioning in asymmetric and symmetric cell divisions (Carminati and Stearns, 1997; McCarthy and Goldstein, 2006; Pecreaux et al., 2006).

The study of the numerous mitotic functions of dynein has been hampered by difficulty in imaging dynein in both fixed and live cells. One of the earliest dynein localization experiments in mammalian cells used a cytoplasmic dynein antibody to show dynein at spindle poles and kinetochores in HeLa and PtK1 cells

fixed with aldehyde (Pfarr et al., 1990). Dynein was first reported to be localized to cortical sites and astral microtubules in fixed mitotic epithelial cells in 1998, using an Arp 1 dynactin antibody and a 70.1 dynein antibody (Busson et al., 1998). These results were reproduced in a different mammalian system, NRK cells, using an intermediate chain antibody, confirming that dynein localized to kinetochores in early prometaphase shifts to astral microtubules and cortical sites in metaphase and anaphase (O'Connell and Wang, 2000). These experiments utilizing immunofluorescent staining reveal dynein complexes on astral microtubules and localized in patches at the cortex in polarized mammalian epithelial cells, implicating dynein as a key player in astral microtubule dependent spindle positioning (Busson et al., 1998). The dynein heavy chain has not been imaged in live mammalian cells, leaving many questions about the dynamic localization of dynein at various stages of mitosis unresolved.

Dynein at the Cell Cortex and Spindle Positioning

The cortical localization of dynein at specific phases of mitosis has been confirmed in mammalian systems by immunofluorescent staining of normal rat kidney (NRK) cells, providing evidence for a model in which cortical dynein positions the spindle via astral microtubules. In the experiment, spindle position was disrupted by physical perturbation, nocodazole treatment and dynein antibody microinjection (O'Connell and Wang, 2000). Misorientation of the spindle caused a delay in anaphase and rotation of the spindle to align with the long axis of the

cell. Fixed cell imaging of nocodozole treated cells revealed a decrease in astral dynein. Cells with inhibited dynein were unable to restore perturbed spindles (O'Connell and Wang, 2000). These results lead to a model whereby dynein, acting on astral microtubules, is responsible for the aligning of improperly oriented spindles (O'Connell and Wang, 2000). The regulation and exact mechanism for dynein dependent force generation on astral microtubules and the cell cortex remain to be characterized in mammalian spindle positioning.

In addition to characterizing the various spindle positioning phenomena observed in a line of mammalian epithelial cells, the goal of this research was to investigate cortical regulatory mechanisms influencing dynein localization to the cortex, where it can exert force to position the mitotic spindle. LLC-Pk1 cells lacking the μ1B subunit of the AP-1B clathrin adaptor complex were found to exhibit unusual spindle positioning phenomena. This line of cells proved a useful investigative tool for focusing on the specific mechanisms that come into play when the spindle is misaligned prior to anaphase, as is the case in a large proportion of LLC-Pk1 cells. LLC-Pk1 cells are a line of immortalized pig kidney epithelial cells generally considered to originate from the proximal renal tubule (Nielsen et al., 1998). Epithelial cells are characterized by their distinct pattern of polarization into apical, basal and lateral domains, and grow within tissues in sheets of columnar, cuboidal or squamous shaped cells resting on a basal lamina (Alberts, 2008). The μ1b subunit of the AP-1B clathrin adaptor complex has been shown to play an important role in basolateral targeting in

LLC-Pk cells, and the AP-1B complex itself defines functionally distinct regions of the cellular membrane (Sugimoto et al., 2002; Folsch et al., 2003).

This research found that asymmetric positioning of the mitotic spindle is observed in about two thirds of cells prior to anaphase onset, followed by differential movement of chromosome bundles in anaphase to recover symmetry. Characterization of spindle positioning in this cell line, combined with future experiments, may elucidate a novel role of dynein or clarify the regulatory pathways surrounding spindle orientation in mammalian epithelium. To investigate the role of cortical dynein in spindle positioning, immunofluorescent fixing and staining was used to localize dynein/dynactin complex in LLC-Pk1α cells. The novel spindle positioning phenomena characterized in LLC-Pk1α cells, which are deficiently polarized due to the missing μ1b subunit, and the comparison of these cells with those expressing the μ1b subunit, suggested a role for the AP-1B clathrin adaptor complex in determining membrane domains related to spindle positioning. Membrane domains determined by the AP-1B clathrin adaptor complex could regulate the localization of dynein to the cell cortex, which in turn plays a role in spindle positioning.

MATERIALS AND METHODS

Cell Culture Methods

LLC-Pk1α cells were cultured in F10-OptiMEM media and grown on coverslips as described by Tulu et al. (Tulu et al., 2006). Selection of LLC-Pk1α cells carrying modified BAC plasmids used F10-OptiMEM media supplemented with 400μg/ml G418. Live imaging of cells on coverslips was performed in Rose chambers using non-CO_2 MEM media. Cells were kept at 37°C while on the microscope. Cell culture and live imaging of LLC-Pk1γ and LLC-Pk-μ1B cell lines was performed as described for the LLC-Pk1α cells.

Spindle Positioning Imaging

Time lapse movies of cultured LLC-Pk1α cells expressing GFP α-tubulin were acquired in phase at 20x with a Hamamatsu Orca ER cooled charge-coupled device camera (Hamamatsu, Bridgewater,NJ) controlled by MetaMorph software (Molecular Devices, Sunnyvale, CA) on a Nikon Eclipse TE 300 microscope with a Perkin Elmer Spinning Disc Confocal Scan head (Perkin Elmer, Wellesley, MA). Cultured LLC-Pk1γ cells expressing GFP γ-tubulin were illuminated with an X-Cite 120 light source (EXFO America, Plano, TX) and a 488 or 568 nm filter cube for imaging at 100 times magnification on the Nikon Eclipse TE 300

microscope setup described above. Phase images of cultured cells of LLC-Pk1-μ1B cells were captured as described above.

Immunofluorescent Fixing and Staining

LLC-Pk1α cells or LLC-Pk-μ1B cells were grown on coverslips until about 30% confluent, and coverslips were rinsed with Ca^{2+} and Mg^{2+} free PBS and fixed in Methanol at –20°C for 7 min or in room temperature Paraformaldehyde for 20 min and HPLC grade Methanol at –20°C for 7 min. After rehydration for 5 min in Ca^{2+} and Mg^{2+} free PBS, coverslips were incubated in a solution of 3% BSA in PBS for one hour at room temperature to prevent nonspecific binding. Coverslips were stained with a 1:100 dilution of Mouse anti-p150 IgG primary antibody (BD Biosciences, Franklin Lakes, NJ) in BSA block for 5 hours at room temperature. After three repetitions of a 10 minute rinse in PBS without agitation, coverslips were stained with a 1:400 dilution of Cy3 (Jackson ImmunoResearch Laboratories, West Grove, PA) conjugated Goat anti-Mouse IgG secondary antibody overnight and another three repetitions of a 10 minute PBS wash were performed. Coverslips were mounted on slides using Vectashield with 4',6-diamidino-2-phenylindole (DAPI) for DNA visualization (Vector Laboratories, Burlingame, CA), sealed with clear nail polish, and stored at 4°C.

Immunofluorescent Imaging

Slides mounted with fixed and stained LLC-Pk1α alpha-tubulin cells or LLC-Pk-μ1B cells were imaged on the Nikon Eclipse TE 300 microscope setup described previously, illuminated with a X-Cite 120 light source (EXFO America, Plano, TX) and a 488 or 568 nm filter cube, and images were acquired with a Hamamatsu Orca ER cooled charge-coupled device camera (Hamamatsu, Bridgewater,NJ) controlled by MetaMorph software (Molecular Devices, Sunnyvale, CA).

Preparation of Images

All images were prepared in Adobe Photoshop version CS4. Original TIFF files are available in unaltered form.

Materials for BAC modification

All dynein constructs were assembled from a dynein heavy chain Bacterial Artificial Chromosome (BAC) called RP23-60K23 from the BACPAC Resource Center. The dynein heavy chain BAC is about 195 kb and includes the entire genomic sequence of *M. musculus* cytoplasmic dynein heavy chain 1, as well as resistance to Chloramphenicol. The Localization and Affinity Purification (LAP) cassette from Tony Hyman is a 2,417 bp sequence containing EGFP from the C-Term R6K-Amp-LAP plasmid with an S-peptide domain for affinity purification.

BAC Modification Methods

The dynein heavy chain BAC RP23-60K23 was modified according to the Gene Bridges Counter-Selection BAC modification kit protocol. A Localization and Affinity Purification (LAP) tag, modified with dynein homology arms, was added in place of the stop codon as described by Muyrers (Muyrers et al., 2004). DH5α *E. coli* carrying the dynein heavy chain BAC RP23-60K23 were cultured from the original stab culture obtained from the BACPAC resource center and purified using the Nucleobond BAC Plasmid purification kit. The purified plasmid DNA was verified with primers BAC 14 and BAC 15 from the Mouse BAC database http://www.mitocheck.org/cgi-bin/BACfinder by PCR and mini-prep with a Qiagen kit according to Warming et al (Warming et al. 2005). Dynein homology arms for either side of the stop codon were added to the LAP cassette using RT-PCR with primers BAC16 and BAC17 following the GeneBridges Counter-Selection BAC Modification Kit.

Competency for homologous recombination was conferred to the verified DH5α bacteria containing the dynein heavy chain BAC by electroporation transformation with the Genebridges pRed/ET plasmid, using Tetracycline to select for transformed bacteria. After induction with L-Arabinose and a temperature shift incubation at 37°C for 1 hour, homologous recombination was performed. Cells were electroporated with 1μL of unpurified PCR product from the LAP cassette homology arm PCR to the bacteria. Colonies that underwent the homologous recombination were selected in Kanomycin and then individual

colonies were grown in liquid cultures and Mini-Prepped for diagnostic PCR analysis.

The product of PCR with primers on either side of the BAC stop codon, BAC14 and BAC13, was run on an agarose gel for detection of colonies with the recombined Dynein Heavy Chain LAP tag construct from the recombined BAC plasmids. A pure colony without un-modified BAC plasmids was selected for Maxi-Prep to purify DNA for Effectene transfection or nucleofection into LLC-Pk1α cells. After transfection or nucleofection with 5μg of purified BAC plasmid DNA, LLC-Pk1α cells were selected in G418 media for two weeks before cloning with cloning rings and plating on cover slips for conformation of expression the transfected plasmid with the modified dynein heavy chain BAC LAP. A western blot was performed after running whole cell extracts of transfected LLC-Pk1α cells on a 4% polyacrylamide gel using Towbin + 0.05% SDS media for the transfer and goat anti-rat GFP antibody and HRP secondary antibody for detection.

The same protocol for BAC modification was repeated to make the dynein heavy chain tail domain construct with the following changes. Homology arms were added to the LAP cassette using primers BAC24 and BAC 17, and verification of the homologous recombination was done on mini-prepped DNA with these same primers. Three constructs were designed for transfection into LLC-Pk1α cells, one full length, one containing just the motor domain and one containing just the tail domain; only the full length and tail constructs were made

using the BAC counter-selection and modification protocol and subsequently transfected or nucleofected into LLC-Pk1α cells.

RESULTS

Phase Contrast Microscopy of Mammalian Epithelial Cells

Novel spindle positioning phenomena were characterized in LLC-Pk1 mammalian epithelial cells by observation with phase contrast microscopy. Time lapse images of LLC-Pk1α cells grown on coverslips until 50-80% confluent and imaged live in Rose chambers at 37°C revealed rotational and translational movements of the chromosomes aligned at the metaphase plate during metaphase. Rotational movement of the metaphase plate greater than 20 degrees was observed in 65.2% of the 23 LLC-Pk1α cells measured with Image J and analyzed in Microsoft Excel for rotation. The metaphase plate was visualized as an organized line of condensed chromosomes as seen in Figure 5b. Of the 23 LLC-Pk1α cells analyzed, the largest rotation observed was 130.9 degrees (Figure 5) and the average rotation during metaphase was 42.6 degrees. The uncompressed 1fps movie created from a series of time lapse images taken every 180 seconds of the LLC-Pk1α cell in Figure 5 appears in the accompanying CD of supplementary data as Movie 1. Among the 15 LLC-Pk1α cells with chromosome rotations over 20 degrees, the average rotation was 61.3 degrees, and the average time spent in metaphase was 21.6 minutes compared to 16.4 minutes in cells without significant rotation. In 73% of the metaphase rotations greater than 20 degrees, the rotation appeared to orient the metaphase plate perpendicular to the long axis of the cell.

A very common observation was a 20-30 degree rotation of the metaphase plate just before entering anaphase, as seen in Movie 2.

Several distinct phenomena of spindle positioning were observed infrequently by phase contrast microscopy of LLC-Pk1α cells. Translational movement of the spindle towards one cortex of the cell followed by translational movement in the reverse direction towards the geometric center of the cell appeared in a handful of the divisions analyzed. These translational movements were termed cortical bumps, and usually occurred just prior to anaphase as seen in Movie 6, however one LLC-Pk1α cell, depicted in Movie 7, displayed two cortical bumps prior to anaphase.

Translational movements observed in LLC-Pk1α cells using phase contrast microscopy were measured in Image J and analyzed in Microsoft Excel. In the 28 LLC-Pk1α cells analyzed for translational metaphase chromosome movements, the position of the metaphase plate at both the beginning and end of metaphase was measured. The frame of the time lapse representing metaphase onset was judged based on observation of chromosome integration to the metaphase plate. The metaphase plate was determined to be symmetric by evaluating a ratio calculated by dividing the metaphase plate position by the length of the long axis of the cell. The long axis of the cell was defined according to the axis along which anaphase movement progressed but measured at anaphase onset. This ratio would equal 0.5 in a cell with a perfectly symmetric spindle located in the exact middle of the cell; the position of the metaphase plate was

categorized as symmetric in cases where the ratio of the metaphase plate position to the cell long axis deviated by less than 5%. In other words, a symmetric spindle was located within the middle 10% of the cell along the long axis. At the beginning of metaphase, marked by chromosome congregation at the metaphase plate, 32.1% of the 28 LLC-Pk1α cells had a symmetric spindle. By the beginning of anaphase, after rotational or translational movement of the spindle during metaphase, only 14.3% of the same 28 LLC-Pk1α cells had a symmetric spindle. For this particular analysis of translational movement, relatively large cells were selected, resulting in a higher percentage of cells with asymmetric spindles. Small cells, especially those that have pulled away from the glass coverslip and rounded up during mitosis, tend to have mitotic spindles positioned more symmetrically within the more compact geometry of the cell.

The movement of each set of daughter chromosomes during anaphase was observed with phase contrast microscopy, measured in Image J and analyzed with Microsoft Excel. Measurements of chromosome movement from the initial position at anaphase onset were used to calculate the absolute distance traveled by translational movement during anaphase for each set of daughter chromosomes in the 93 LLC-Pk1α cells observed. These 93 LLC-Pk1α cells were placed into two categories based on the position of the metaphase plate at anaphase onset. The metaphase plate position was quantified using the same ratio described previously, by dividing the distance of the metaphase plate from one cortex by the long axis of the cell, with 0.5 representing perfect symmetry with the metaphase

plate centered in the middle of the cell. Of the 93 LLC-Pk1α cells analyzed, only about a third had a mitotic spindle aligned in the middle 10% of the cell at anaphase onset, while 61.3% had an asymmetric spindle at anaphase onset.

In the set of mitotic cells with asymmetric spindles at anaphase onset, 63.2% showed greatly unequal movements of each set of chromosomes with one set of chromosomes traveling at least twice as far as the other. Only 5.7% of the cells with a symmetric spindle at anaphase onset had one chromosome bundle move more than twice as far as the other. Figure 6 depicts the absolute distance traveled for each set of chromosomes, also referred to as chromosome bundles, for both the symmetric and asymmetric sets of mitotic cells. Each set of daughter chromosomes is assigned a letter, with the set of daughter chromosomes originating from the side of the metaphase plate that is closest to the cell cortex referred to as chromosome bundle A. Chromosome bundles assigned the letter A, shown in purple, travel less far for both symmetric and asymmetric data sets. For the mitotic cells categorized as symmetric, the set of chromosomes originating on the side of the metaphase plate closest to the cortex traveled an average of 6.1 μm, compared to an average of 8.1 μm for the 'B' chromosomes farther from the cell cortex. Of the 63.2% of LLC-Pk1α cells with an asymmetric spindle at anaphase onset, the average distance traveled by the 'A' chromosomes was 4.4 μm, less than half of the average distance traveled by the 'B' chromosomes, which was 10.7 μm.

The division in Movie 3 is typical of the asymmetric divisions observed in 63.2% of LLC-Pk1α cells, and frames from this movie are shown in Figure 7. The long edge of the chromosomes aligned along the metaphase plate in Figure 7b is initially positioned parallel to the long axis of the cell, but metaphase rotational movement positions the metaphase plate more perpendicular to the long axis in Figure 7d, the frame representing anaphase onset. During anaphase in Figure 7e through h the set of daughter chromosomes towards the top of the frame travels farther than the set of daughter chromosomes closer to the cell cortex.

The symmetry of the daughter cells in relation to the position of the spindle at anaphase onset was quantified in 28 LLC-Pk1α cells by measuring the position of the cleavage plane between the two daughter cells. The symmetry of both the metaphase plate just prior to anaphase and the cleavage plane was assessed by calculating the ratio of their position over the length of the long axis of the cell. Again, a ratio equaling 0.5 represented perfect positioning at the midpoint of the long axis, and cells with metaphase plate or cleavage plane position within the middle 10% of the cell were considered symmetric. At anaphase onset, 89.7% of the LLC-Pk1α cells analyzed had an asymmetric metaphase plate as defined according to the ratio described above. By cytokinesis, 72.4% of those same LLC-Pk1α cells had a cleavage plane positioned at the center of the two dividing daughter cells. In the specific example of the LLC-Pk1α cell depicted in Figure 7 and Movie 3, the ratio of symmetry calculated for the metaphase plate is 0.363, a significant deviation from the

midpoint of the cell. By cytokinesis, the ratio calculated for the symmetry of the cleavage plane along the new long axis of the cell is 0.454, within the middle 10% of the cell deemed to be symmetric. The apparent unequal size of the daughter cells in the two dimensional phase contrast images is potentially a misleading marker of symmetry due to the three dimensional nature of these cells, although the ratio of symmetry does indicate that the cleavage plane was not exactly symmetric, instead deviating by just less than 5% of the total length of the cell.

The asymmetry observed in LLC-Pk1α cells, and the representative cell depicted in Figure 7, was quantified by tracking the position of the chromosomes over time during both metaphase and anaphase. A graph of these measurements from the time lapse represented in Movie 3, shown in Figure 8, reveals migration of the metaphase plate to about 5μm off center from the middle of the long axis of the cell. The asymmetry observed at anaphase onset is countered by differential migration of each chromosome bundle, with chromosome bundle B traveling nearly 3 times as far as chromosome bundle A. This drastic difference in the anaphase movement of each chromosome bundle results in relatively symmetric daughter cells despite the asymmetry of the spindle at anaphase onset, as seen the frames in Figure 7. The relative symmetry of the daughter cells is difficult to visualize in the two dimensional images taken from time lapse movies, but was more apparent when examined on the microscope by focusing on various levels of the three dimensional cell.

Fluorescent Microscopy of Centrosomes in Mammalian Epithelial Cells Expressing Fluorescent Gamma Tubulin

To confirm that the asymmetric position of the mitotic spindle at anaphase onset and the unequal movements of the chromosomes during anaphase observed in phase contrast correspond to movements of the entire mitotic spindle, time lapse movies in both phase and fluorescence were taken of LLC-Pk1γ cells. LLC-Pk1γ cells are genetically modified to express γ-tubulin labeled with GFP, but are otherwise the same as the LLC-Pk1 and LLC-Pk1α cell lines. The centrosomes at either pole of the mitotic spindle, which organize the microtubules of the mitotic spindle in animal cells, contain γ-tubulin. The centrosomes are readily apparent in LLC-Pk1γ cells and the bright dots mark the spindle pole throughout mitosis as seen in the frames in Figure 10. The frames in Figure 10 represent the phase contrast (Figure 10a-h) and corresponding fluorescent images (Figure 10a'-h') collected throughout mitosis in an LLC-Pk1γ cell. Although the particular cell shown in Figure 10 has an uneven border, the long axis of the cell can still be determined according to the axis along which anaphase progresses, and the spindle is located asymmetrically along that axis at anaphase onset, depicted in Figure 10d and Figure 10d'. Also visible in the frames selected from the time lapse series with fluorescent images taken every 30s are oscillations of the spindle. These oscillations are readily apparent in Movie 5.

The fluorescent movie of an LLC-Pk1γ cell in Movie 5 shows the positioning of the spindle and the movement of the spindle poles in anaphase. A

kymograph of the spindle poles tagged with GFP γ-tubulin in the same LLC-Pkγ cell is shown in Figure 11. The border of the cell is visible due to the subpopulation of cytoplasmic GFP γ-tubulin, while the dark shadow of the chromosomes represents the void of fluorescent γ-tubulin. The spindle poles are represented by the bright white spots of GFP fluorescence from the confluence of γ-tubulin at the centrosomes. Both the spindle poles and the daughter chromosomes clearly have different trajectories. The spindle pole on the right is seen to move for a small period of time just after anaphase onset, the beginning of the kymograph, and then remain in the same spot. In contrast, the spindle pole to the left continues to move throughout anaphase and after cytokinesis begins, moving significantly farther during the course of the division.

Immunofluorescent Fixing and Staining of LLC-Pk1α Cells

Immunofluorescent fixing and staining was used to determine the localization of dynein throughout mitosis in LLC-Pk1α cells. In fixed LLC-Pk1α cells lacking the μ1b subunit of the AP-1B clathrin adaptor complex, dynein was localized with a p150 antibody to detect dynactin. Dynactin antibodies are commonly used to reveal dynein localization, as dynein is only rarely found in a cell without the dynactin complex (Karki and Holzbaur, 1999; Gaetz and Kapoor, 2004; Myers et al., 2007). The 100x magnification fluorescent images in Figure 12 depict the typical staining observed for prophase LLC-Pk1α cells, with the GFP microtubules seen in green fluorescence in Figure 12a. A maximum

projection of a Z-stack captured in the red fluorescence channel in Figure 12b shows p150 antibody for dynactin labeled with red Cy3. The color combined image in Figure 12c reveals red p150 antibody on the tips of spindle microtubules. These microtubules were confirmed to be kinetochore microtubules by localization of DNA with DAPI labeling, not shown. A typical metaphase LLC-Pk1α cell is represented by Figure 13, again with microtubules in Figure 13a and p150 dynactin antibody in Figure 13b. The color combined image in Figure 13c reveals a pool of dynactin, and presumably dynein, at the far end of the cell from the asymmetrically positioned spindle. In 94% of the live LLC-Pk1α cells observed, metaphase spindles positioned closer to one end of the cell signaled anaphase onset. Therefore it can be assumed that this cell, had it not been fixed, would have proceeded to anaphase shortly after the point captured in Figure 13.

Early in anaphase, LLC-Pkα cells generally contained a cortical ring of dynactin localized opposite the asymmetrically positioned spindle, as represented in Figure 14, where the void in the cytoplasmic pool of GFP labeled α-tubulin reveals the chromosomes just beginning to separate. Staining for p150 is noticeably absent from the cell cortex closest to the asymmetrically positioned spindle in Figure 14.

Late in anaphase or early telophase, as the cleavage furrow is beginning to form, cortical p150 dynactin staining is still apparent in both the maximum projection (Figure 15b) and in a frame selected from the p150 Z-stack (Figure 15c) of the LLC-Pkα cell in Figure 15. The cortical p150 staining is significantly

increased in one end as opposed to the other, although it is impossible to tell from this fixed cell whether the spindle was positioned farther from that cortex at anaphase onset. Telophase LLC-Pkα cells imaged from fixed and stained coverslips generally appeared similar to the telophase cell in Figure 16, which shows no cortical p150 dynactin staining at the cortex in both the p150 (Figure 16b) and color combined (Figure 16c) images. Instead, p150 dynactin staining labels the tips of microtubules in the late telophase cell in Figure 16, which is similar to the plus end staining of microtubules observed in fixed interphase cells.

The cortical, kinetochore and plus-end localization of dynactin as revealed by staining with p150 antibody in fixed LLC-Pk1α cells grown on coverslips was quantified by scoring over 200 fixed and stained LLC-Pk1α cells. The results of this scoring are shown in Figure 17, and confirm that dynein/dynactin is present at the cortex opposite spindles positioned asymmetrically at the opposite cortex in about 90% of LLC-Pkα cells at anaphase onset or in metaphase with an asymmetric spindle. Furthermore, the cortical localization of dynactin appears to be highly dependent upon the phase of mitosis, as it is generally absent in prophase, metaphase and at cytokinesis.

Phase Contrast Microscopy of LLC-Pk-μ1B Cells

To compare the LLC-Pk-μ1B cells expressing the μ1B subunit of the AP-1B clathrin adaptor complex to the LLC-Pk1α cells lacking this membrane protein, anaphase spindle position and daughter cell symmetry was assessed. The

symmetry of the daughter cells in relation to the position of the spindle at anaphase onset was quantified in 13 LLC-Pk-μ1B cells by measuring the position of the cleavage plane between the two daughter cells. The symmetry of the metaphase plate just prior to anaphase and the cleavage plane was assessed by calculating the ratio of their position over the length of the long axis of the cell. As described previously, a ratio equaling 0.5 represented a position at the exact midpoint of the long axis, and cells with metaphase plate or cleavage plane within the middle 10% of the cell were categorized as symmetric. At anaphase onset, 61.5% of LLC-Pk-μ1B cells exhibit a metaphase plate positioned at the midpoint of the cell as defined according to the ratio described above. By cytokinesis, 76.9% of the LLC-Pk-μ1B cells analyzed had a cleavage plane positioned at the center of the two dividing daughter cells.

Tracking the movement of the chromosomes through metaphase and anaphase in a representative LLC-Pk-μ1B cell confirmed the relative symmetry suggested by the measurements above. The progression of mitosis in the LLC-Pk-μ1B cell pictured in Movie 4 is representative of the typical cell division observed in this cell line. A 71 degree rotation is observed during metaphase to align with the long axis of the cell. The measurements of chromosome position collected in Image J from metaphase to telophase are graphed in Figure 8b. The trajectory of the chromosomes revealed in this graph displays minimal deviation from the midpoint of the cell during metaphase and symmetric movements of each set of daughter chromosomes during anaphase.

Different patterns of spindle orientation and anaphase movement of each spindle pole are easily compared with kymographs. Kymographs place a segment of each frame from a time lapse sequence of images one after another with time on the vertical axis to show movement over time within that strip of the time lapse. A kymograph from a phase movie of an LLC-Pk-µ1b cell is shown in Figure 9b, while a kymograph from a phase movie of an LLC-Pk1α cell appears in Figure 9a. A frame from the corresponding time lapse movies appears to the right of the kymograph to show the area represented in the kymograph. The dark chromosomes can be seen to move in very symmetric trajectories in the first kymograph of an LLC-Pk-µ1b cell. In the LLC-Pk1α cell in Figure 9a the dark chromosomes of the metaphase plate move off center during metaphase. In anaphase, each set of daughter chromosomes has a distinctly different trajectory. The chromosome bundle on the side closer to the cell cortex moves very little, the opposite chromosome bundle on the left of Figure 9a travels quickly and moves farther.

DISCUSSION

The characterization of spindle positioning phenomena in a line of mammalian epithelial cells revealed a pattern of asymmetric spindle position at anaphase onset followed by unequal movement of each set of sister chromatids in a significant subpopulation of cells. In addition to phase contrast observation of spindle positioning, microscopic observation of mammalian epithelial cells expressing fluorescent gamma tubulin revealed asymmetric movement of each spindle pole during anaphase. Immunofluorescent fixing and staining of mammalian epithelial cells suggested a spindle positioning role for dynein located at the cell cortex. Mammalian cells with and without the μ1b subunit of the AP-1B clathrin adaptor complex were compared to determine whether this polarizing membrane protein could play a role in spindle positioning.

The primary conclusion reached by careful characterization of the movement of the mitotic spindle in mammalian epithelial cells is that the location of the spindle remains extremely plastic throughout the phases of mitosis. Rotational and translational movement was observed during metaphase, and analysis revealed variation in the resulting position of the spindle at the end of metaphase. The rotational movements observed in LLC-Pk1α cells were significant in changing the alignment of the mitotic spindle within the geometry of the cell, as the average rotation was over 40 degrees and more than 65% of the

cells had a rotation greater than 20 degrees. The minimum rotation of 20 degrees was chosen as a cutoff point to represent significant rotation of the mitotic spindle based on the definition of proper spindle alignment as within 20 degrees from the long axis in literature on the subject (O'Connell and Wang, 2000). A significant (greater than 20 degree) rotation placed the axis of the spindle parallel to the long axis of the cell in 73% of divisions. These findings lead to the conclusion that rotation of the metaphase plate to position the spindle for division is a common mechanism for metaphase alignment of the spindle in LLC-Pk1α cells. In addition, this outcome agrees with previous work to determine the preferred spindle position in relation to cellular geometry in a similar mammalian cell line (O'Connell and Wang, 2000).

A study of spindle positioning in normal rat kidney (NRK) cells found that the spindle preferentially aligned such that the pole to pole axis was parallel to the long axis of the cell (O'Connell and Wang, 2000). Direct rotation of the spindle was observed in cases where the spindle was improperly oriented (O'Connell and Wang, 2000). The rotation of the spindle in response to the geometric space defined by the cortex of the cell implies that the dynamic microtubules and microtubule associated proteins of the mitotic spindle can in some way integrate spatial information and react. Within the subpopulation of 65% of LLC-Pk1α cells with rotations greater than 20 degrees, the average time spent in metaphase was 21.6 minutes, compared to 16.4 minutes in cells without significant rotation. The O'Connell and Wang study corroborated previous work showing that

incorrect orientation of the mitotic spindle, necessitating rotation to align with the long axis, resulted in delayed anaphase (O'Connell and Wang, 2000). A delay could give evidence for the role of a spindle positioning checkpoint in mammalian cells, which has been characterized in yeast (O'Connell and Wang, 2000). The position of the spindle may be related to a mitotic checkpoint, causing a delay in anaphase onset when spindle position does not satisfy certain requirements.

Furthermore, the rotational movement observed in the majority of LLC-Pk1α cells, over 65 percent, reflects the dynamic interaction between astral microtubules and the cell cortex. The cell division depicted in the uncompressed movie (Movie 2) of an extreme rotation is 180 times faster than real time, yet the drastic rotation observed within a three minute time interval exemplifies the active interaction between the cytoskeleton with the geometry of the cell. A study investigating the involvement of PAR proteins in microtubule dynamics at the cortex of *C. elegans* embryos recorded an average microtubule contact of 14.5 and 16.5 seconds at the anterior and posterior cortex respectively (Labbe et al., 2003). The brevity of cortical contacts relates to models of spindle positioning with astral microtubules, and sheds light into the dynamic movements of the spindle observed during metaphase.

One previously uncharacterized phenomenon of spindle movement observed in LLC-Pk1α cells is the translational movement of the metaphase plate towards the cell cortex. Although these distinct cortical bumps occurred in relatively few of the cells analyzed, understanding these movements could

provide insight into the mechanism of spindle positioning during metaphase, as well as the interaction of astral microtubules and the cell cortex. The translational movements, seen in Movie 6, usually occurred just prior to anaphase, as with many of the rotations discussed previously. These cortical bumps, and the dividing cell which displays two cortical bumps during metaphase in Movie 7, raise the question of the degree of randomness of metaphase spindle positioning.

Analysis of translational movement during metaphase in 28 LLC-Pk1α cells revealed that translational movements during metaphase generally did not move the metaphase plate towards the center of the cell. While 32.1% of the cells started with a symmetric spindle at the beginning of metaphase, by the end of metaphase only 14.3% of the same cells had a symmetric spindle. For this particular analysis of translational movement, relatively large cells were selected, resulting in a higher percentage of cells with asymmetric spindles. Small cells, especially those that have pulled away from the glass coverslip and rounded up during mitosis, tend to have mitotic spindles positioned more symmetrically within the more compact geometry of the cell. Regardless of the disproportionately high number of asymmetric cells stemming from inability to analyze mitosis in small cells that have rounded up, these observations point to an interesting trend in metaphase spindle movements.

The mechanism and function of the cortical bumps described in LLC-Pk1α cells, consisting of translational movement towards one cortex of the cell during metaphase, remain unknown. In meiotic divisions in fission yeast, nuclear

oscillations along the long axis of the cell are generated by an uneven distribution of dynein motors anchored to the cell cortex (Tolic-Norrelykke, 2010). These cortical dynein motors pull on microtubules as they walk towards the minus end, and their uneven localization within the cell creates a greater force on the long leading microtubules until the nucleus reaches the cortex and the leading microtubules shorten, at which point the motion changes direction (Tolic-Norrelykke, 2010). Dynein at the cell cortex interacting with astral microtubules could generate the force required for the translational movements observed in LLC-Pk1α cells, but the purpose of these movements towards the cell cortex is unclear.

Measurement of the speed of these translational movements could confirm the identity of the motor protein involved in these cortical bumps and such measurements are an avenue of future research. Because there is no apparent function for the translational movement observed in a small population of LLC-Pk1α cells, it is difficult to draw a conclusion about the significance of these metaphase movements; they may very well represent random movement of the spindle. What does emerge from this research is the observation that although rotational movement during metaphase tends to orient the spindle along the long axis of the cell for division, the translational movement of the chromosomes does not in general enhance the symmetry of the metaphase plate.

Spindle positioning has been described previously in normal rat kidney (NRK) cells; the spindle was said to ‘always’ be located ‘near’ the geometric

center of the cell (O'Connell and Wang, 2000). The phase contrast observation of LLC-Pk1α cells conducted revealed a striking departure from both the widely accepted model for symmetric cell division and the well characterized NRK cell pattern of spindle positioning. Symmetric cell divisions are generally attributed to placement of the metaphase plate at the midpoint of the long axis of the cell followed by equal movements of each set of daughter chromosomes during anaphase (Grill and Hyman, 2005; Alberts, 2008). In contrast, only 37% of the 93 LLC-Pk1α cells analyzed had a spindle positioned symmetrically along the long axis just prior to anaphase as defined by the stringent cutoff of the middle 10% of the cell. This larger data set included more cells with a smaller total area, and consequently has a more representative, higher percentage of cells with symmetric spindles than the population of cells analyzed for translational movement during metaphase. These results reveal that the majority of LLC-Pk1α cells begin anaphase with a mitotic spindle that is not located centrally in the cell.

The asymmetric position of the mitotic spindle at anaphase onset is often considered a determining factor in asymmetric cell divisions such as the well characterized one-cell-stage *C. elegans* embryo. In a review of asymmetric spindle positioning, McCarthy Campbell et al. describe the correlation between spindle position and daughter cell size: “When a mitotic spindle becomes positioned asymmetrically within a cell, cell division results in daughter cells that are unequal in size” (McCarthy and Goldstein, 2006). Following this logic, we could hypothesize that a significant portion of the LLC-Pk1α cells with an

asymmetric spindle at anaphase onset would produce unequal daughter cells. To test this hypothesis, the position of the cleavage plane resulting from constriction of the actin cytoskeleton ring during cytokinesis was compared to the position of the metaphase plate prior to anaphase.

Inquiry into the potential connection between asymmetric spindle positioning and unequal size of daughter cells focused on the position of the cleavage plane in cytokinesis. The cleavage plane was selected as a marker of symmetry for daughter cells because of the challenge posed in assessing the three-dimensional size of daughter cells through the two-dimensional information gleaned from phase contrast microscopy. Focusing through the three-dimensional structure of live cells while on the microscope confirmed that daughter cells with a symmetric cleavage plane were relatively equal in size. Again, a smaller data set representing the larger subpopulation of LLC-Pk1α cells was used in this analysis, resulting in a high proportion of spindles positioned asymmetrically at anaphase onset. Of the 28 LLC-Pk1α cells analyzed, 89.7% had an asymmetric metaphase plate just prior to anaphase, as defined according to the ratio described previously. Contrary to the stated hypothesis, 72.4% of those same LLC-Pk1α cells had a cleavage plane positioned evenly at the center of the two dividing daughter cells by cytokinesis. Despite a very high proportion of asymmetric spindles at anaphase onset, the majority of the daughter cells resulting from these supposedly asymmetric divisions were in fact symmetric. The apparent contradiction of cell division dogma exposed in this analysis of LLC-Pk1α cells

implies that a mechanism must exist to correct for the position of asymmetric spindles and give rise to equal daughter cells.

Careful analysis of the movement of each set of daughter chromosomes throughout anaphase, observed with both phase contrast and fluorescent microscopy, shed light on the corrective mechanism at play in LLC-Pk1α cells. The unknown mechanism appeared to assure equivalent daughter cells even in cases where cell division proceeded from an asymmetrically positioned spindle. The division of the LLC-Pk1α cell shown in Movie 3 and graphed in Figure 8a gives an excellent example of this phenomenon observed in a significant portion of the cell line. The ratios of symmetry calculated for both the metaphase plate and the cleavage plane reveal that the asymmetric spindle at anaphase onset was corrected, with the cleavage plane positioned within 5% of the center of the cell at cytokinesis. During anaphase, the graph in Figure 8a depicting the movement of each set of daughter chromosomes gives a clue to the mechanism behind this recovery of symmetry. The anaphase movement of each chromosome bundle follows a different trajectory, with the chromosome bundle closest to the cortex of the cell moving about a third of the distance traveled by the other set of daughter chromosomes in the same amount of time.

The movement observed in this cell is not anomalous, in fact this asymmetry in anaphase movement of the chromosomes is almost universal among cells starting anaphase with an asymmetric spindle, as shown by the cumulative data presented in Figure 6 from the 93 LLC-Pk1α cells analyzed for anaphase

chromosome movement. Within the set of cells in which cell division began anaphase with an asymmetric spindle, as defined previously, one set of chromosomes traveled more than twice as far as the other on average. The prominent difference in the trajectories of each set of daughter chromosomes, depending on their initial distance from the cortex, implies the existence of a mechanism that can direct differential movement of each spindle pole, relative to the geometry of the cell, during anaphase.

In order to make the conceptual link from the movements of the chromosomes observed via phase contrast microscopy to the entire mitotic spindle, fluorescent microscopy of LLC-Pk1 cells expressing fluorescent gamma tubulin was used to visualize the spindle poles. Gamma tubulin makes up the pericentriolar material of the centrosomes, which organize the microtubules of the mitotic spindle into two poles. Kymograph analysis of the movement of the centrosomes during anaphase in LLC-Pk1γ cells revealed different trajectories for each centrosome, paralleling the differential movement of the chromosomes observed in the larger data set of LLC-Pk1α cells. Observation of the centrosomes, the organizational hubs of the spindle microtubules, by fluorescent microscopy confirmed that the asymmetric anaphase movement of each set of daughter chromosomes stemmed from a spindle microtubule based mechanism. With the spindle position and movement phenomenon well characterized by phase contrast observation now established as a microtubule dependent phenomenon of

the entire spindle, the question of the mechanism behind this phenomenon can be evaluated.

A microtubule length dependent model of spindle positioning by dynein located at the cortex neatly explains how a cell could in effect sense the position of the mitotic spindle, while at the same time providing the mechanism for moving the spindle to the center of the cell. In a discussion of spindle positioning by cortical pulling forces such as dynein, Stephan Grill and Anthony Hyman point out that a model of length-dependent forces could correlate spindle position with the geometry of the cell (Grill and Hyman, 2005). The model states that longer microtubules have the potential to interact with more motor proteins to generate greater force on the side of the spindle furthest from the cortex, repositioning the spindle in the center of the cell. Cortical contact with microtubules along a significant length of the cell in order to interact with motors located at the cell cortex requires a relatively flat cell. The LLC-Pk1α cells used in this research tend to remain flat throughout mitosis, although some cells do round up and become considerably three-dimensional, especially depending upon confluence of the cultured cells. It seems plausible that cortical motor proteins could generate length dependent forces on astral microtubules in the relatively flat epithelial cells used in this investigation, and this model has been suggested as an explanation for spindle positioning in NRK cells, a line of mammalian epithelial cells also derived from the kidney (O'Connell and Wang, 2000; Grill and Hyman, 2005).

To determine whether dynein motor proteins generating force at the cell cortex could play a role in the spindle positioning phenomenon observed in LLC-Pk1α cells, immunofluorescent fixing and staining with anti-p150 antibody was used to localize dynactin. Dynactin colocalizes with dynein and antibodies raised against dynactin have been widely used for immunofluorescent detection of dynein (Karki and Holzbaur, 1999; Gaetz and Kapoor, 2004). The immunofluorescent fixing and staining performed in this research revealed consistent accumulation of dynactin antibody at the plus ends of microtubules in interphase cells. At all phases of mitosis from prophase to telophase, dynactin antibody stained the mitotic spindle, including kinetochore and interpolar microtubules as well as the plus ends of astral microtubules. A cytoplasmic pool of dynein was also apparent in all cells. These results are consistent with previous research that localized dynein in mammalian epithelial cells (Busson et al., 1998; O'Connell and Wang, 2000).

In prophase, LLC-Pk1α cells fixed and stained with dynactin antibody displayed kinetochore accumulation of dynactin, as seen in Figure 12. The localization of dynein/dynactin to the kinetochores during prophase and prometaphase is consistent with prior dynein localization experiments in mammalian cells (Busson et al., 1998). The ability to reproduce earlier immunofluorescence experiments indicated that the method of fixing and staining was sensitive enough to detect dynein complexes with specific localization to mitotic structures

In metaphase, cortical patches of dynactin staining appeared in agreement with prior experiments (Busson et al., 1998; O'Connell and Wang, 2000). However, previous immunofluorescent experiments to localize dynein did not find asymmetric distribution of cortical staining, which appeared in a significant portion of the fixed and stained metaphase cells analyzed in this investigation (Busson et al., 1998). In the majority of cases in which a metaphase spindle was positioned asymmetrically, dynactin staining was apparent at the far end of the cell, enhanced in the cytoplasm and/or along the far cortex. The localization of accumulations of dynein/dynactin at cortical sites opposite spindles positioned off of the midpoint of the long axis of the cell implies that dynein could generate the cortical pulling forces necessary to realign the spindle in the geometric center of the cell.

During anaphase, cortical localization of dynein/dynactin was also found to be asymmetric in several cases, again corresponding with an asymmetric spindle and appearing at the opposite end of the cell. Dynein/dynactin staining was reduced in telophase as the mitotic spindle was dismantled, although cells were still observed to have some dynactin on the mitotic spindle with rare cortical patches. In the late stages of cytokinesis, dynactin antibody was undetectable on microtubules except at the plus ends. Localization of dynein through immunofluorescent fixing and staining with dynactin antibody reveals asymmetric distribution of dynein/dynactin motor complexes.

These complexes of motor protein positioned opposite misaligned metaphase mitotic spindles seems significant in light of the carefully characterized phenomenon of asymmetric spindle position and unequal anaphase chromosome movement in this line of cells. Dynein motor complexes on the cortex of the cell could walk along long astral microtubules and generate force in the correct direction to pull a mitotic spindle from the far end of the cell back towards the middle. In fact, this model of force generation has been demonstrated to cause meiotic nuclear oscillations that pull the spindle from one end of the cell to the other in fission yeast (Tolic-Norrelykke, 2010).

Studies in model systems such as budding yeast and *C. elegans* have implicated dynein as an important generator of the cortical forces necessary for spindle positioning (Carminati and Stearns, 1997; Kozlowski et al., 2007). There are several different mechanisms that could explain the role of cortical dynein in spindle positioning. A study by McCarthy and Goldstein (2006) describes the cortical forces on microtubules that determine spindle positioning and direct asymmetrical cell divisions and suggest that these processes could also be mediated by dynein (McCarthy and Goldstein, 2006). In addition, dynein-dependent interactions with microtubules at the cell cortex function to orient the spindle in budding yeast *S. cerevisiae*, and G-protein signaling is known to function with dynein to position the spindle in *C. elegans* early embryos (Carminati and Stearns, 1997; Couwenbergs et al., 2007). Because membrane-associated Gα protein is known to regulate dynein, and is widely implicated as a

cortical force generator, it follows that other membrane-associated or cortical protein interactions could be involved in the localization of dynein to the cell cortex.

The exact mechanism by which various proteins including cytoplasmic dynein collaborate to position the mitotic spindle relative to the cell's geometry remains unknown in mammalian cells, although dynein has been implicated in several other model systems. A study quantifying the relationship of spindle elongation to cell size in *C. elegans* early embryos found that spindle elongation appears to be controlled by both Gα-dependent and independent mechanisms represented by a force-generator-limited model involving dynein or constant-pulling model, respectively (Hara and Kimura, 2009). Gα protein is one of the membrane bound subunits of trimeric G protein, which relays signals from G-protein-linked receptors, an abundant class of cell-surface receptor. The two models of spindle regulation are supported by data showing that both the speed of spindle elongation and the subsequent spindle length after anaphase elongation correlate with cell size (Hara and Kimura, 2009). Gα protein and Gα protein regulator knockdown with RNAi uncoupled the relationship between the speed of spindle elongation and cell size, in addition to disrupting full elongation of the spindle (Hara and Kimura, 2009). The Gα-dependent mechanism implicated in the Force-generator-limited model includes dynein complexes at the cell cortex recruited by G-proteins to pull on microtubules (Hara and Kimura, 2009). G-protein dependent regulation of dynein at the cell cortex gives a hint as to how the

cell membrane, the cytoskeleton of the cell cortex and the motor proteins and cytoskeleton of the mitotic spindle could be related.

The cell membrane is made up of heterogeneous domains with different biochemical and functional characteristics. Epithelial cells grow in sheets resting upon a basal lamina, and are cuboidal, columnar or squamous in shape with polarized apical, basal and lateral domains (Alberts, 2008). The LLC-Pk1 epithelial cell line was isolated from pig kidneys in the 1950s and was later recognized to originate from the proximal renal tubule, which is made up of simple cuboidal epithelium. Epithelial cells that are columnar or cuboidal in shape generally position the mitotic spindle in the apical region of the cell, and dynein/dynactin is known to localize in a ring below the tight junction, where conserved PAR proteins which regulate cell polarity accumulate (Ahringer, 2003). The cuboidal shape is not preserved when LLC-Pk1 cells grow on glass or plastic, instead the cells grow in a flat monolayer (Hull et al. 1976). An interesting avenue of investigation lies in performing similar observations and analysis of spindle positioning in LLC-Pk1 cells growing on Transwell polycarbonate membrane, which promotes growth of polarized layers of epithelial cells. Immunofluorescent fixing and staining of LLC-Pk1 cells that were grown in a polarized epithelial layer more representative of epithelial morphology within a tissue could clarify the distribution of proteins known to regulate spindle position in polarized cells and shed light on their role in spindle positioning. Despite the difference between epithelial cell growth within a tissue and the

cultured structural characteristics of LLC-Pk1 cells, LLC-Pk1 cells remain an interesting model system within which phenomena of cell division can be investigated. The molecular details of the mechanism for orienting the mitotic spindle in mammalian epithelial cells can be teased out through work in cell lines such LLC-Pk1 cells, and membrane domain regulatory proteins, as well as PAR proteins, G-proteins and dynein, remain areas to explore in relation to the spindle positioning phenomena characterized in this work.

A 2007 study by Toyoshima and Nishida revealed a mechanism involving integrin to orient the mitotic spindle of nonpolarized mammalian cells parallel to the substrate independent of gravity and cell-cell adhesion (Toyoshima and Nishida, 2007). Integrin spans the membrane to interact with both extracellular matrix proteins such as fibronectin and collagen as well as the intracellular actin cytoskeleton (Toyoshima and Nishida, 2007). The microtubule plus end tracking protein EB1 stabilizes the plus end of microtubules, while myosin X remodels the actin cytoskeleton (Toyoshima and Nishida, 2007). The mechanism proposed for parallel spindle orientation relies on the interaction of integrin with both the extracellular matrix and the intracellular cytoskeleton via myosin X and EB1, a cortical interaction with astral microtubules that is also known to be mediated by dynein (Toyoshima and Nishida, 2007). These models of spindle position and size regulation are particularly relevant to our discussion of spindle positioning in LLC-Pk1 cells, a line of mammalian epithelial cells missing the AP-1B clathrin adaptor subunit μ1B.

Many important cellular processes rely on the differentiation of membrane domains, which can change in response to environmental or intracellular cues. The AP-1B clathrin adaptor complex subunit μ1B is essential for targeting to the basolateral surface, and is not present in LLC-Pk1 cells (Sugimoto et al., 2002). LLC-Pk1 cells are derived from pig kidney epithelium and display a flat morphology generally maintained throughout mitosis, facilitating imaging (Hull et al., 1976). Because they lack the baso-lateral targeting function associated with μ1B, the μ1B deficient LLC-Pk1 cell line is described as defectively polarized (Folsch et al., 2003). Because of this defect, cultured LLC-Pk1 cells do not represent the normal function of proximal tubule cells within living tissue, but their importance as a model system for studying the mechanism of spindle positioning is undiminished. The AP-1A and AP-1B clathrin adaptor complexes play a role in distinguishing membrane domains that could explain regulation of dynein localization at the cortex in mammalian cells (Folsch et al., 2003). Cortically localized PAR proteins have been shown to regulate the dynamics of microtubules in *C. elegans*, and display asymmetric localization in human cells that could play a role in spindle positioning and asymmetric cell division (Labbe et al., 2003). These membrane defining proteins could be related to dynein through G-protein pathways similar to those described by Hara and Kimura in 2009. The connection is exemplified by the differential localization of G-proteins during asymmetric cell division in *C. elegans* and *Drosophila*, under the regulation of the PAR proteins (Sugimoto et al., 2002).

To begin the investigation of the role of membrane proteins in the particular spindle positioning phenomenon of LLC-Pk1α cells described by this research, LLC-Pk1α cells were compared to LLC-Pk-μ1B cells modified to express the μ1B subunit. Initial results from the quantification of anaphase spindle position and daughter cell symmetry in 13 LLC-Pk-μ1B cells suggest that mammalian epithelial cells with the μ1B subunit do not display the spindle positioning phenomenon described in LLC-Pk1α cells, although more research must be done to reach a conclusion on this subject. Primary data from the LLC-Pk-μ1B cells determined that over 60% of cells exhibit a metaphase plate positioned at the midpoint of the cell at anaphase onset, and that by cytokinesis, 76.9% of the LLC-Pk-μ1B cells analyzed had a cleavage plane positioned at the center of the two dividing daughter cells. An initial assessment of these data implies a greater rate of symmetry at anaphase onset in mammalian epithelial cells with the μ1B subunit. Although the kymograph analysis of the LLC-Pk-μ1B cell presented in Figure 9b represents only one cell, the initial data from 13 LLC-Pk-μ1B cells suggest that the differential trajectories of each set of daughter chromosomes observed during anaphase in LLC-Pk1α cells may not occur commonly in cells with the μ1B subunit.

To solidify the conclusions reached from this very preliminary data on the role of the μ1B subunit of the AP-1B Clathrin Adaptor Complex, many more LLC-Pk-μ1B cells must be observed and analyzed in a manner similar to that used for the LLC-Pk1α cells. Further experiments could include a comparison of the

time spent in metaphase for LLC-Pk cells with and without the μ1B subunit. These measurements could prove whether polarization of the baso-lateral domains of the cell membrane plays a role in spindle positioning, and make conclusions about the potential for a spindle positioning checkpoint in mammalian epithelial cells. Further comparison of dynein localization in LLC-Pk cells with and without the μ1B subunit must be carried out using both immunofluorescent fixing and staining and techniques for imaging fluorescent proteins in live cells. A comparison of LLC-Pk cells with and without the μ1B subunit growing on Transwell polycarbonate membrane to promote polarization of the epithelial layer and subsequent fixing and staining with antibodies for dynein and Gα protein would also be enlightening.

Much work remains to be done in order to understand the complex interaction of membrane domains, regulatory proteins, motor proteins and the cytoskeleton that determines spindle position and chromosome movement in mammalian epithelial cells. In particular, localization of dynein in live mammalian cells with fluorescent tags would provide essential information about the temporally and spatially specific role of dynein throughout mitosis. Preliminary work was done to express *Mus musculus* dynein heavy chain tagged with fluorescent EGFP at endogenous levels in mammalian cells with Bacterial Artificial Chromosome (BAC) technology. The primary advantage to using a BAC vector for molecular manipulation of mammalian cells is the large size of the vector, which allows transfection and expression of the entire genomic

sequence of dynein including all introns and the promoter and regulatory sequences. The use of the original dynein promoter in transfected cell lines means that dynein can be expressed at endogenous levels after siRNA or RNAi knockdown experiments, eliminating questions about whether the level of expression is affecting phenotypes. The initial groundwork to engineer constructs of the dynein heavy chain in a BAC vector using homologous recombination and electroporation was completed successfully (results unpublished), but transfection into mammalian cells was unsuccessful.

The molecular localization of dynein with BAC technology in live cells would allow precise visualization of dynein using *in vivo* fluorescent microscopy that will be more accurate and informative than the immunofluorescent techniques used in this work and in most prior studies. BAC technology in conjunction with RNAi has been established as an accurate and efficient technique for performing knock-down experiments or testing mutant phenotypes (Kittler et al., 2005). The molecular fluorescent localization of dynein would answer questions about where dynein localizes at different phases of mitosis as well as the dynamics of the motor protein's movements throughout the spindle and cortex of a mitotic cell.

The detailed description of the metaphase and anaphase spindle phenomena observed in LLC-Pk1α cells provides insight into an important model system within which mechanisms for spindle positioning can begin to be elucidated. Further research to localize dynein heavy chain in live cells and to test the role of membrane regulatory proteins and signaling proteins such as Gα-

proteins will shed light on the important details of this complex process. Understanding the myriad proteins and cellular processes involved in distinct aspects of cell division remains an important goal of scientific research, as cell division itself is fundamental to development, reproduction, healing, aging, and cancer.

FIGURES

Figure 1. Phase Contrast Images of Mitosis in a Mammalian Epithelial Cell

Images selected from a 20x phase time-lapse series showing a mammalian epithelial cell in mitosis. Image a shows a prometaphase LLC-Pk1α cell with condensed chromosomes. A metaphase LLC-Pk1α cell with chromosomes aligned at metaphase plate is shown in b, while image c is of an LLC-Pk1α cell in anaphase A. The image in d shows an LLC-Pk1α cell in anaphase B with cleavage furrow apparent.

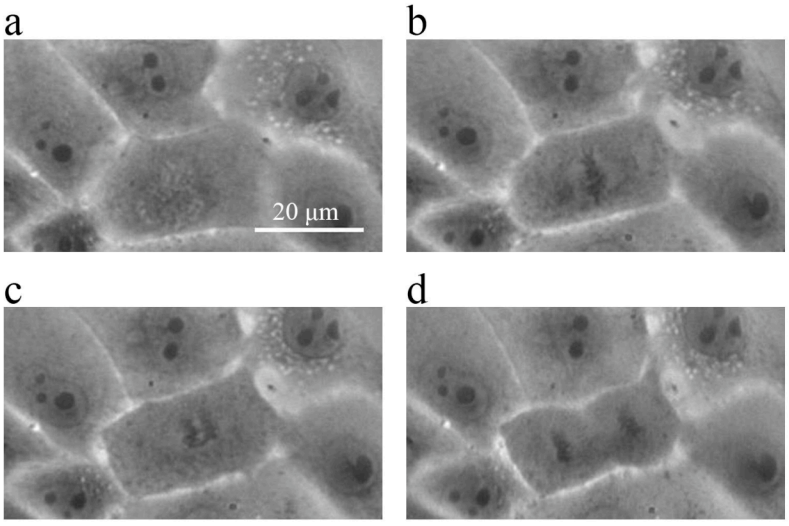
a
b
20 µm
c
d

Figure 2. Fluorescent Images of Mitosis in a Mammalian Epithelial Cell

Fluorescent micrographs of live LLC-Pkα cells at 100x expressing GFP conjugated α-tubulin reveal the structure of spindle microtubules during mitosis. Prometaphase is shown in image a, and image b is of metaphase with long astral microtubules visible. Anaphase showing astral microtubules and elongated interpolar microtubules is shown in image c. (Nick Ferenz)

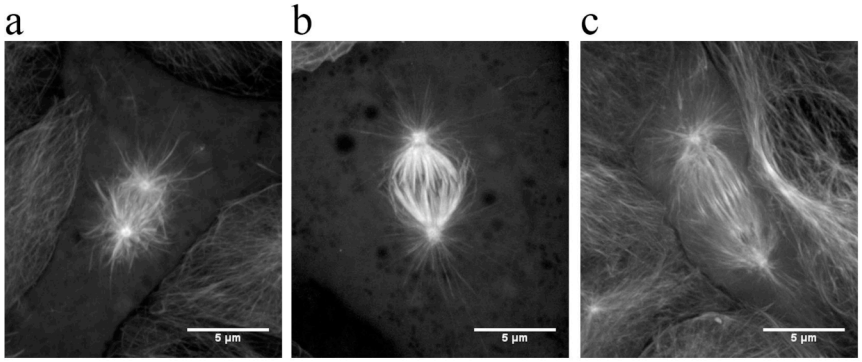
a
b
c
5 µm
5 µm
5 µm

Figure 3. Gennerich and Vale Diagram of Dynein Protein Domains

Diagram of the cytoplasmic dynein heavy chain homodimer and associated subunits from Gennerich and Vale showing the microtubule binding domains (MTBDs), coiled-coil regions and AAA domains at the C-terminus of each heavy chain (Gennerich and Vale 2009).

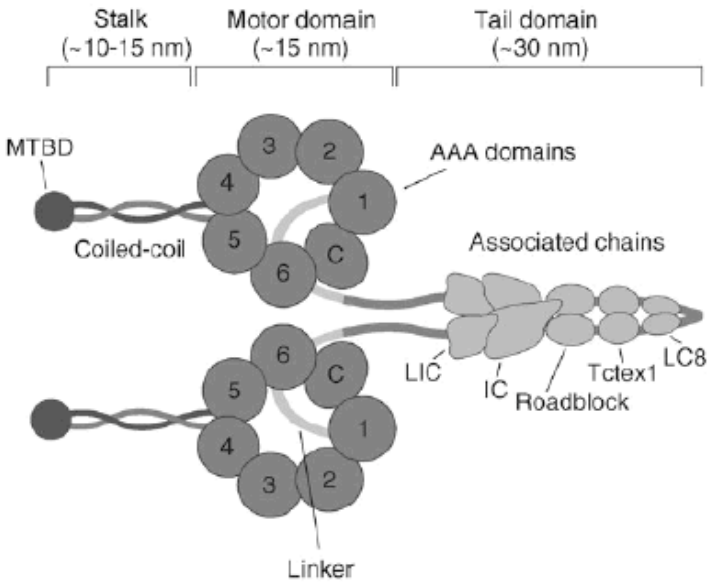
Stalk
(~10-15 nm)
Motor domain
(~15 nm)
Tail domain
(~30 nm)
MTBD
Coiled-coil
AAA domains
Associated chains
LIC
IC
Roadblock
Tctex1
LC8
Linker

Figure 4. Diagram of Dynein Protein Domains from King Data

Diagram of the functional domains of the dynein heavy chain amino acid sequence compiled from data published by Stephen King. The diagram shows the location of the tail and motor domains including the six AAA domains with ATPase activity and the microtubule binding domain (King 2000).

Mouse Cytoplasmic Dynein Heavy Chain Protein Map

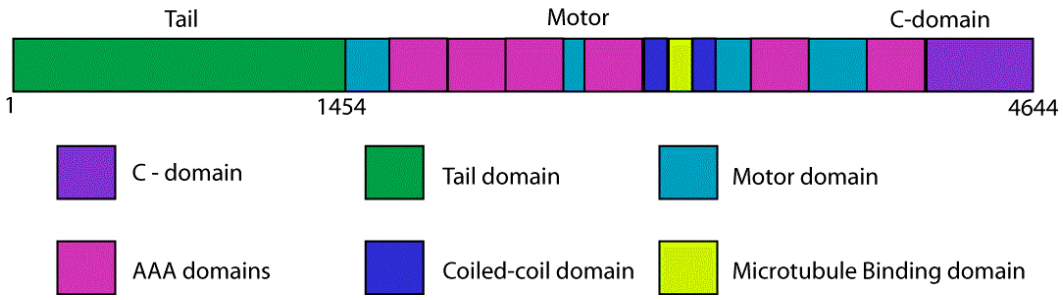

Figure 5. Rotation of the Metaphase Plate in an LLC-Pk1α Cell

Figure 5 depicts direct rotation of the chromosomes organized on the metaphase plate, with prophase shown in image a, anaphase onset represented in image g and telophase beginning in image i. Images were selected from a 20x phase contrast time lapse series of live LLC-Pk1α cells with images captured every 180 seconds.

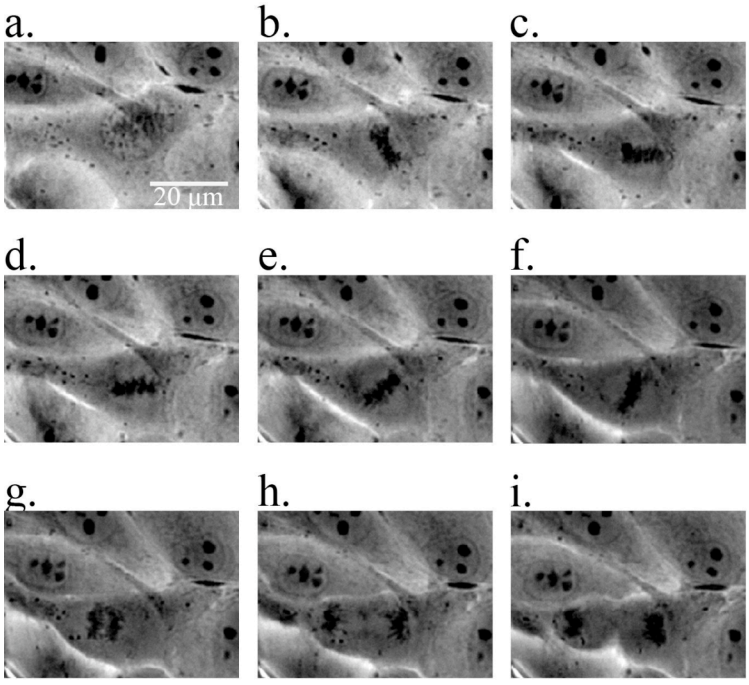
a.
b.
c.
20 µm
d.
e.
f.
g.
h.
i.

Figure 6. Anaphase Chromosome Movement in LLC-Pk1α Cells

These absolute distances of translational movement are graphed for each set of sister chromosomes for each mitotic cell in either the symmetric or asymmetric data set. The average distance traveled for each set of chromosomes appears at the end of the data set. The mitotic cells categorized as symmetric appear in part a. while the mitotic cells categorized as asymmetric appear in part b.

a

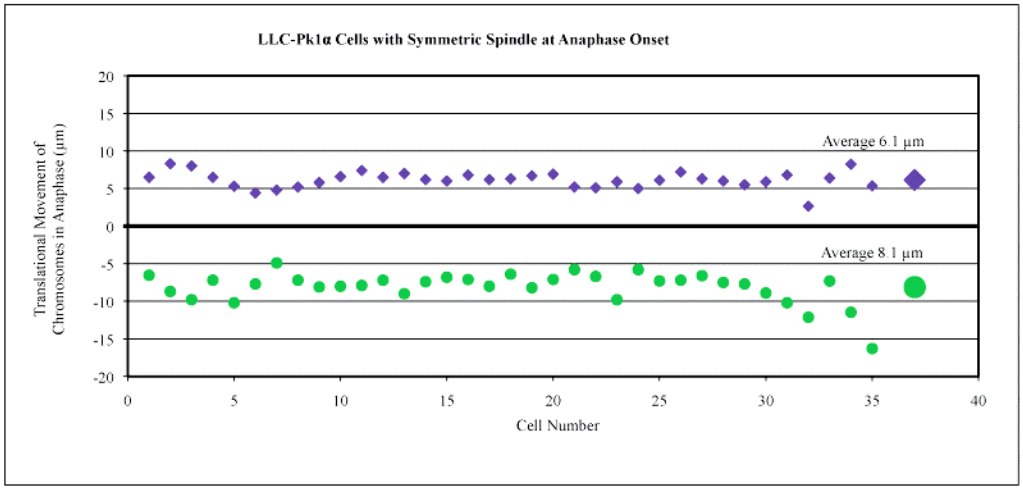
LLC-Pk1α Cells with Symmetric Spindle at Anaphase Onset
Translational Movement of Chromosomes in Anaphase (µm)
Average 6.1 µm
Average 8.1 µm
Cell Number

b

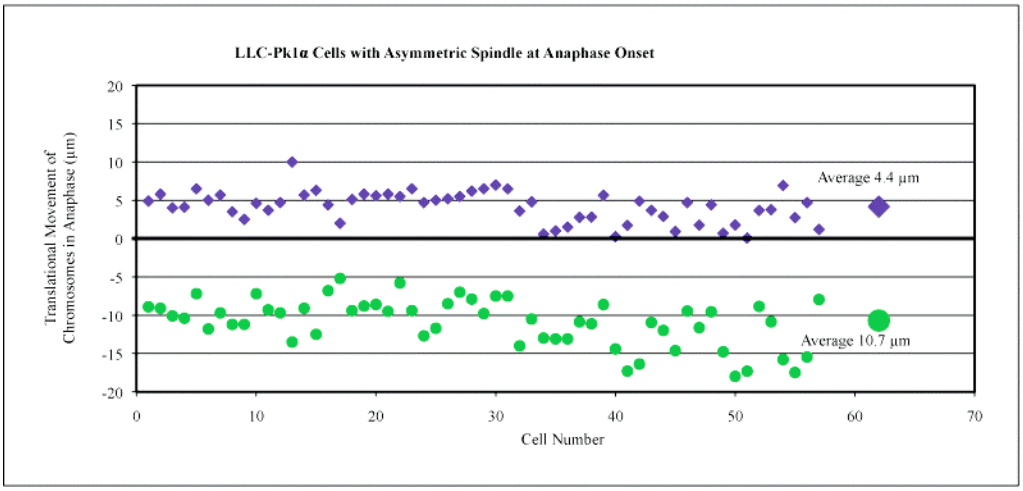
LLC-Pk1α Cells with Asymmetric Spindle at Anaphase Onset
Translational Movement of Chromosomes in Anaphase (µm)
Average 4.4 µm
Average 10.7 µm
Cell Number

Figure 7. Phase Contrast Images of Mitosis in an LLC-Pk1α Cell

Select images from a time lapse movie taken in phase at 20x magnification of LLC-Pk1α cells cultured on coverslips and imaged in a Rose chamber at 37°C. Frames b-d depict metaphase spindle rotation to align with the long axis of the cell, and asymmetric spindle position at anaphase onset is shown in frame d.

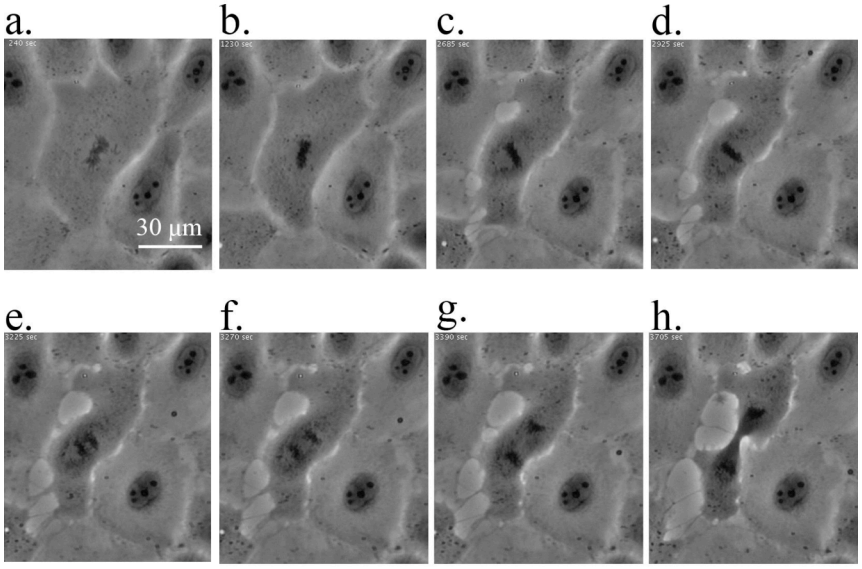
a.
b.
c.
d.
240 sec
1230 sec
2685 sec
2925 sec
30 µm
e.
f.
g.
h.
3225 sec
3270 sec
3390 sec
3705 sec

Figure 8. Tracking Chromosome Position

Graphs depict the relative position of chromosome bundles from metaphase onset to the end of anaphase, as measured in Image J. Measurements for part a are from a time lapse movie of an LLC-Pkα cell grown on a coverslip and imaged in a Rose chamber at 37°C, captured in phase at 100x magnification. Measurements for part b are from a phase contrast time lapse movie of an LLC-Pk1-μ1B cell grown on a coverslip and maintained in a Rose chamber at 37°C during imaging every 15 seconds at 100x magnification.

a

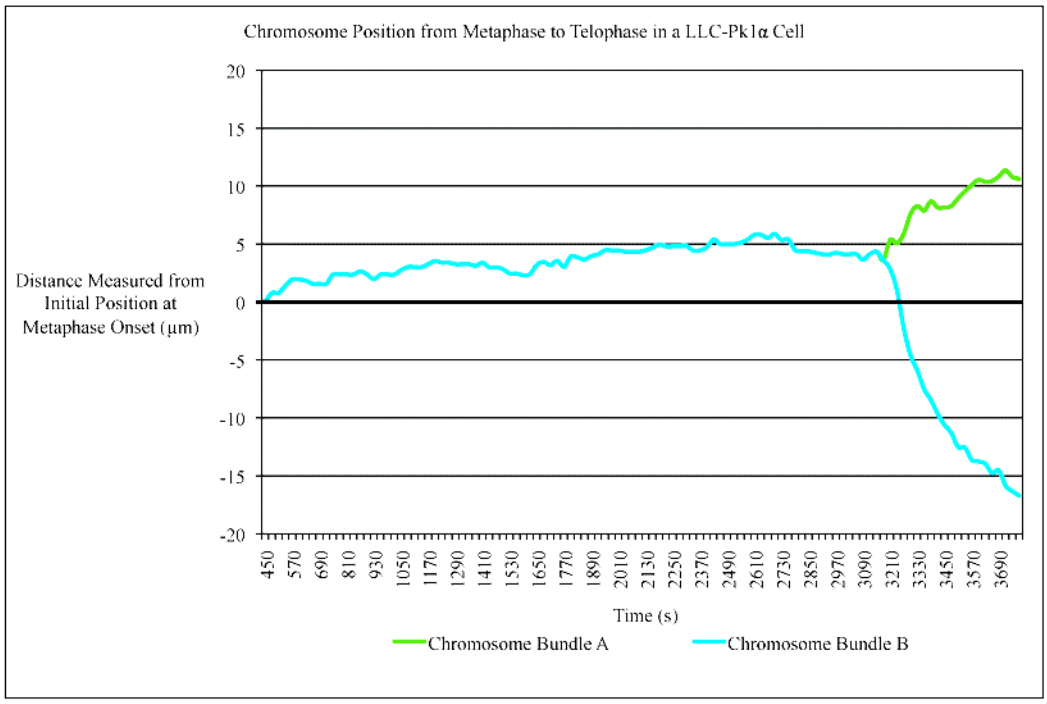
Chromosome Position from Metaphase to Telophase in a LLC-Pk1α Cell
Distance Measured from Initial Position at Metaphase Onset (µm)
20
15
10
5
0
-5
-10
-15
-20
450
570
690
810
930
1050
1170
1290
1410
1530
1650
1770
1890
2010
2130
2250
2370
2490
2610
2730
2850
2970
3090
3210
3330
3450
3570
3690
Time (s)
Chromosome Bundle A
Chromosome Bundle B

b

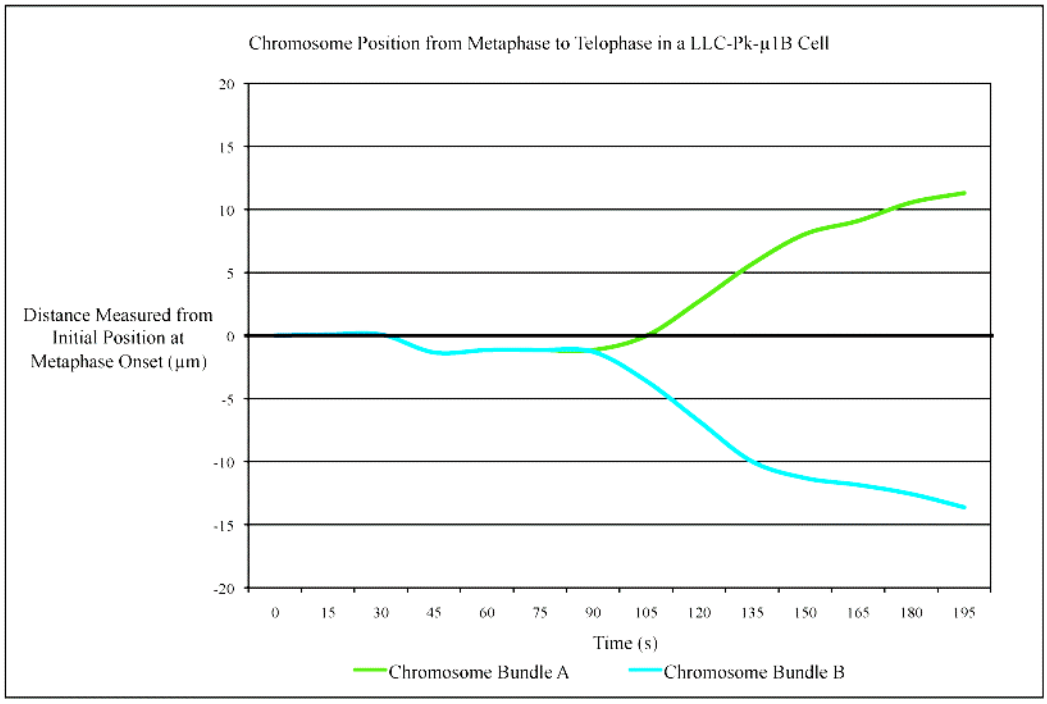
Chromosome Position from Metaphase to Telophase in a LLC-Pk-µ1B Cell
Distance Measured from Initial Position at Metaphase Onset (µm)
20
15
10
5
0
-5
-10
-15
-20
0
15
30
45
60
75
90
105
120
135
150
165
180
195
Time (s)
Chromosome Bundle A
Chromosome Bundle B

Figure 9. Kymograph Analysis of Chromosome Movement

Kymographs of an LLC-Pk-mu1B and an LLC-Pkα cell appear in parts a and b respectively, with a frame from the corresponding time lapse appearing to the right to show the section represented by the kymograph. The midpoint of the cell, the borders of the cell, and the times of anaphase and cytokinesis onset are labeled.

a

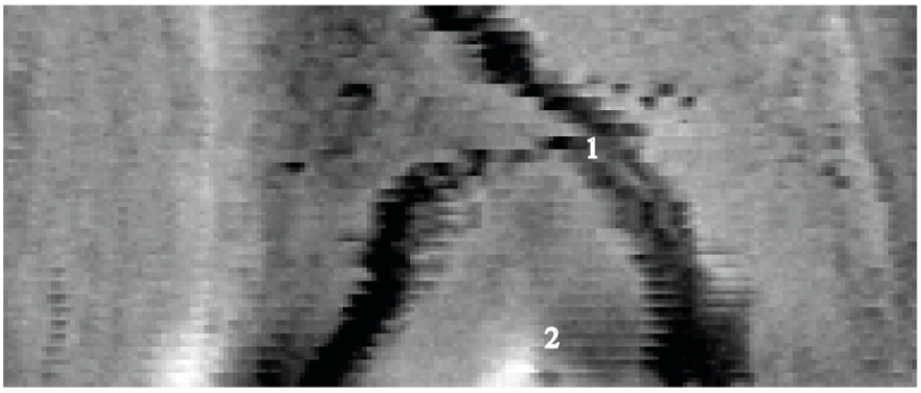

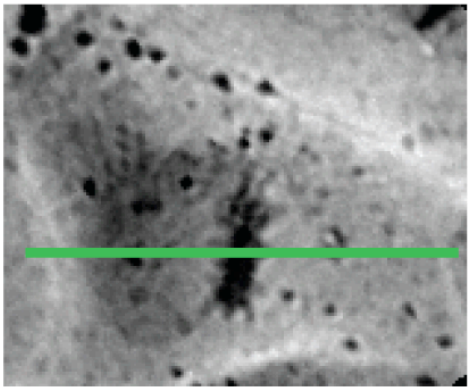

b

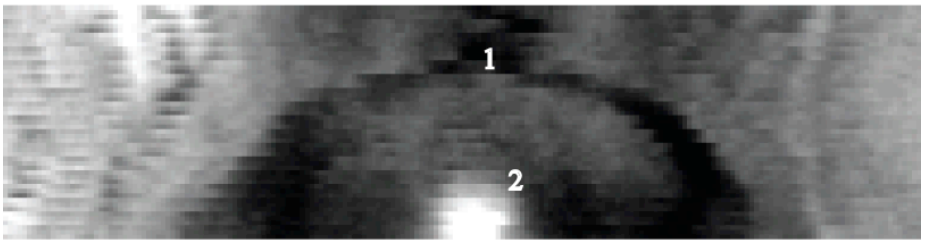

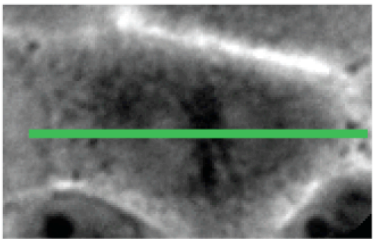

Figure 10. Centrosome Observation during Mitosis in an LLC-Pk1γ Cell

Phase contrast images selected from a time lapse series with images captured every 30 seconds of an LLC-Pk1γ cell are shown in a-h, while the corresponding fluorescent images of GFP γ-tubulin labeling the centrosomes to localize the spindle poles are in a'-h'. LLC-Pk1γ cells were cultured on coverslips and imaged at 37°C in a 30s time lapse.

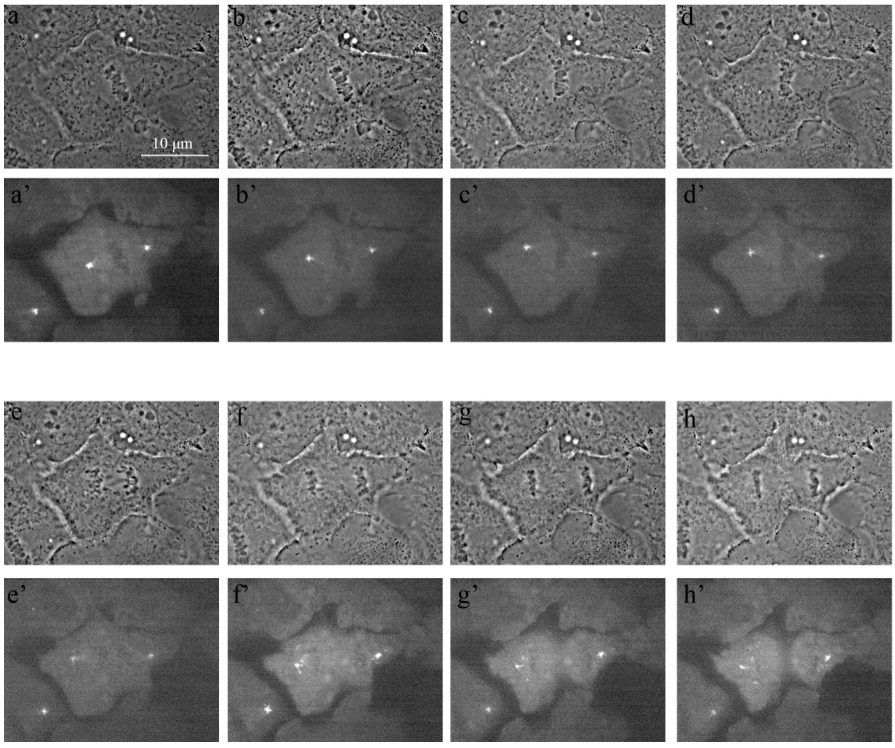
a
b
c
d
10 µm
a'
b'
c'
d'
e
f
g
h
e'
f'
g'
h'

Figure 11. Analysis of Centrosome Movement in an LLC-Pk1γ Cell

A kymograph with time on the vertical axis was made in Image J from the region shown in the frame in part b, which was selected from the time lapse movie of this LLC-Pkγ cell. The midpoint of the cell, the borders of the cell, the centrosomes, the void of the chromosomes and the times of anaphase and cytokinesis onset are labeled.

a

b

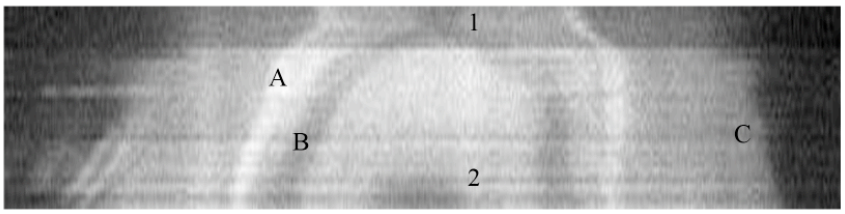

c

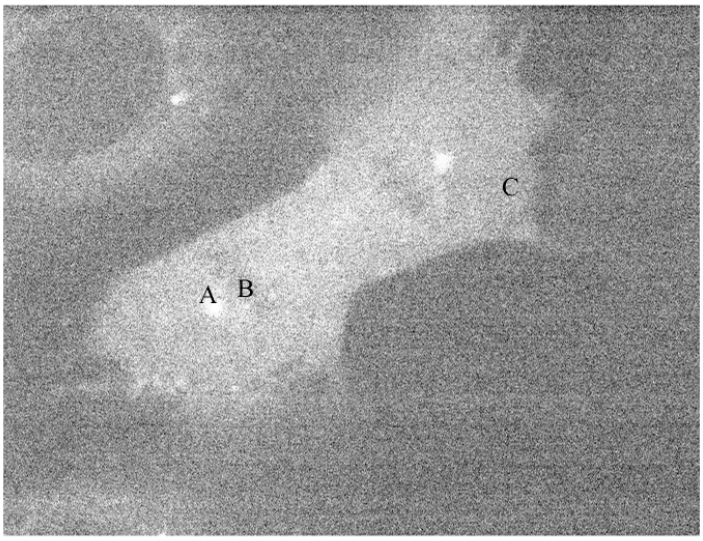

d

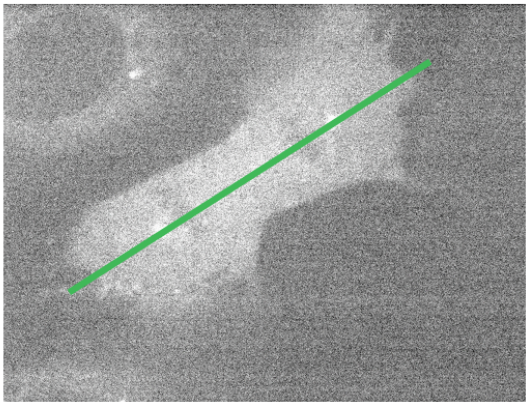

Figure 12. Dynactin Localization in a Prophase LLC-Pk1α Cell

Immunofluorescent fixing and staining with p150 antibody revealed dynactin in a prophase LLC-Pk1α cell in image b, a maximum projection of a Z-series of fluorescent images. Image a shows fluorescent microtubules, and image c shows the color combined overlay of the two images to reveal dynactin localized to the kinetochores.

a.

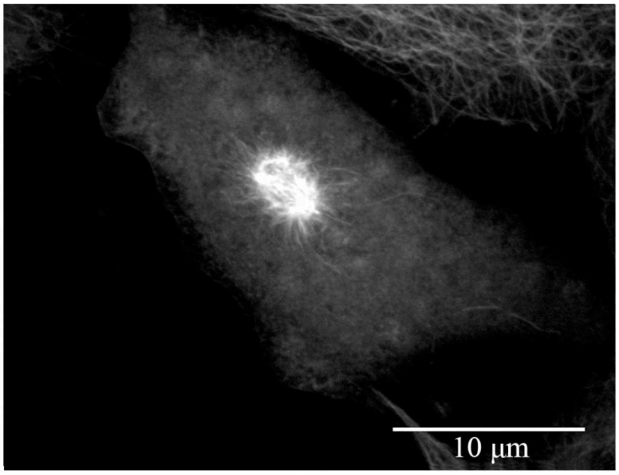

b.

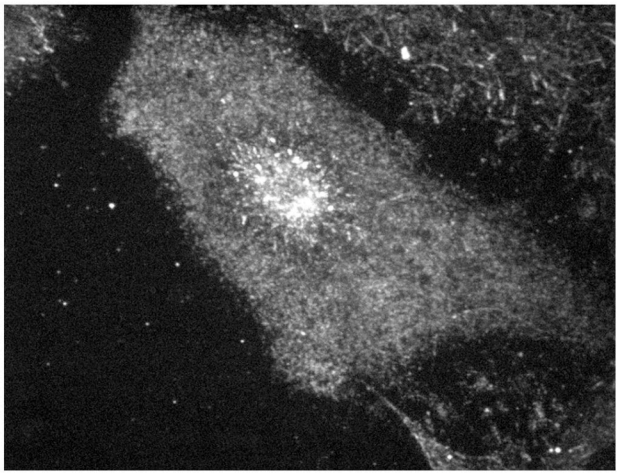

c.

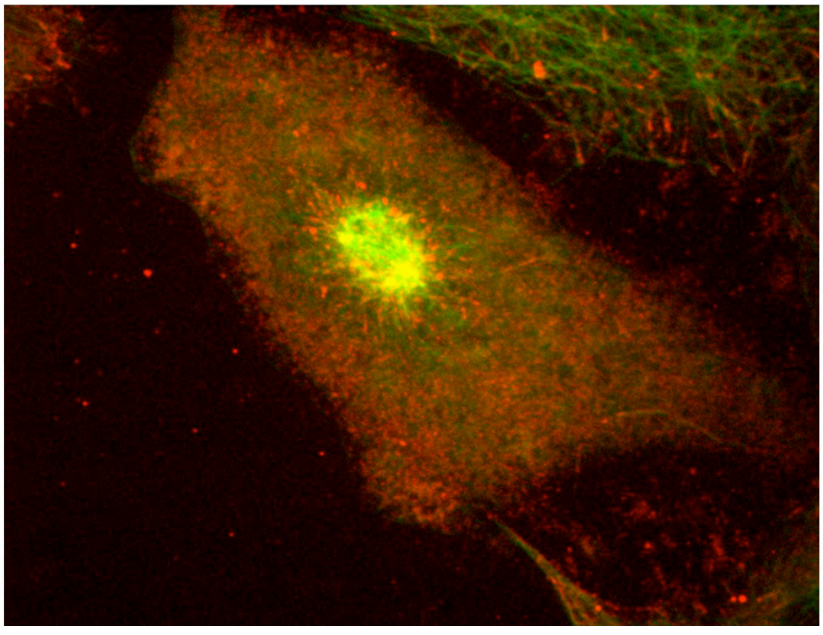

Figure 13. Dynactin Localization in a Metaphase LLC-Pk1α Cell

Immunofluorescent fixing and staining with p150 antibody revealed dynactin localization in a metaphase LLC-Pk1α cell as shown in the maximum projection in image b, with a single image selected from the p150 z-series shown in image c. Fluorescent microtubules in image a show an asymmetric spindle, and image c shows the color combined overlay of the two images depicts dynactin at the far end of the cell from the asymmetric spindle, as well as dynactin on the mitotic spindle and at plus ends of astral microtubules.

a.

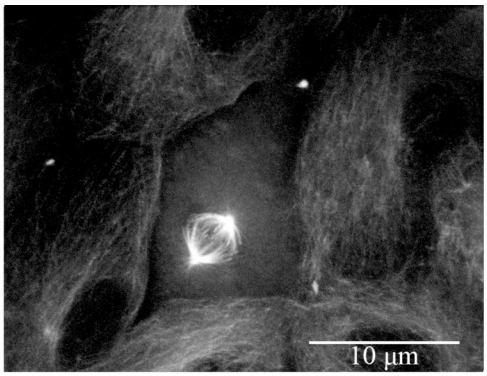

b.

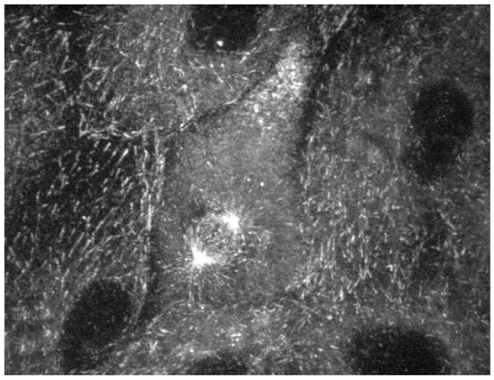

c.

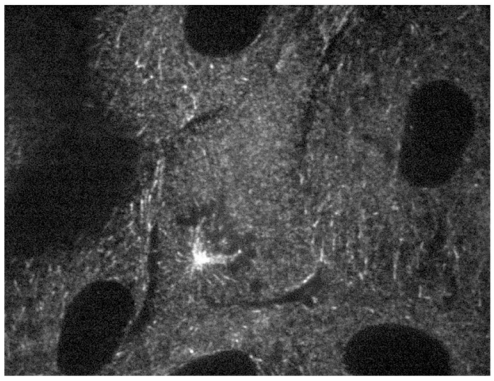

d.

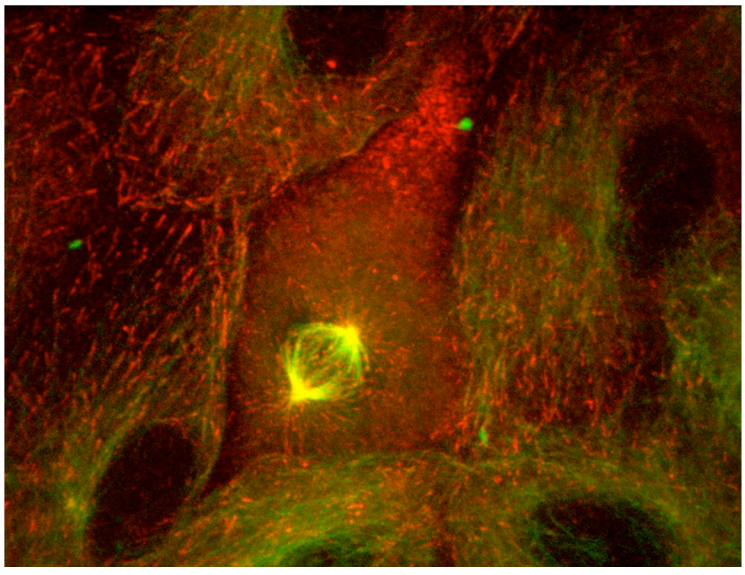

Figure 14. Dynactin Localization in an Anaphase LLC-Pk1α Cell

The maximum projection of fluorescent microtubules in a fixed and stained anaphase LLC-Pk1α cell in image a shows copius astral microtubules and a slightly elongated anaphase spindle closer to the left cortex. Image b, the maximum projection of p150 staining, reveals cortical dynactin at the far right end of the cell from the asymmetric spindle on the left side. The color combined overlay of the two images in image c shows some dynactin localized to the spindle.

a.

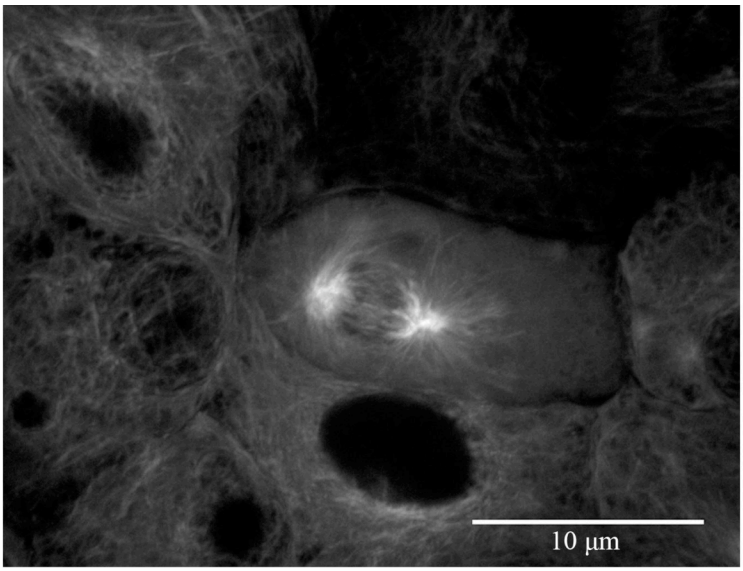

b.

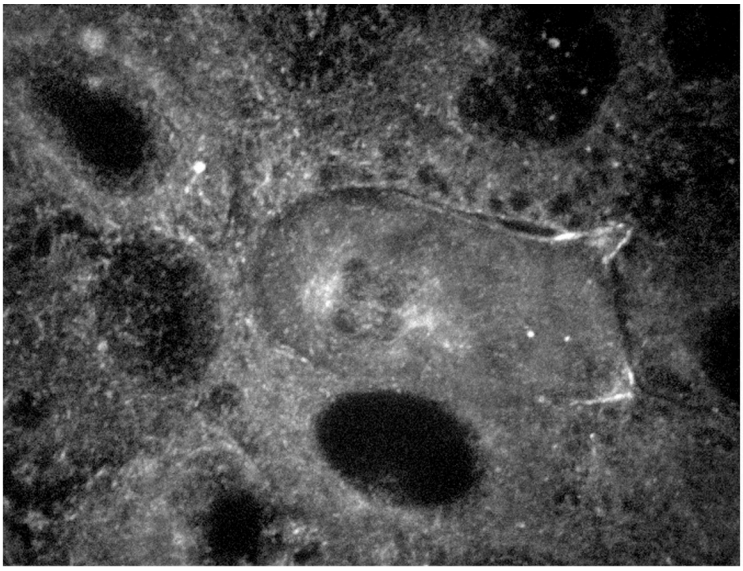

c.

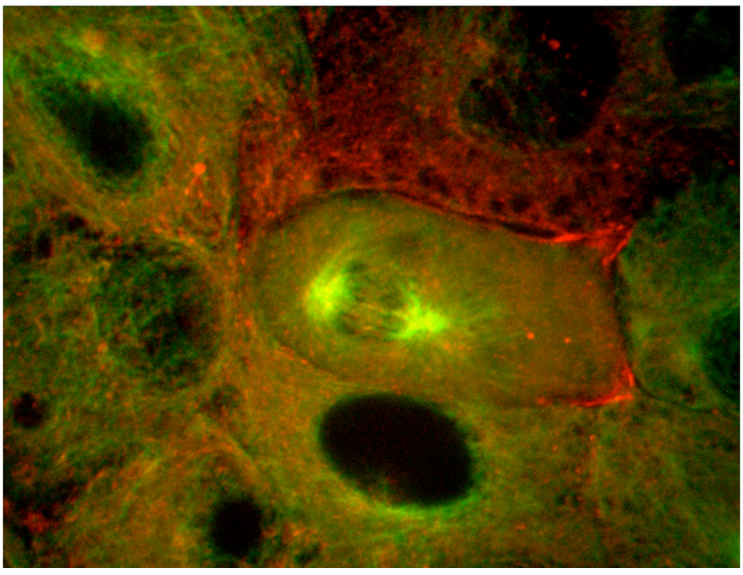

Figure 15. Dynactin Localization in a Telophase LLC-Pk1α Cell

Immunofluorescent fixing and staining with p150 antibody revealed dynactin localization to the cortex in a telophase LLC-Pk1α cell as shown in the single frame selected from the p150 z-series in image c. Fluorescent microtubules in image a show a very elongated late anaphase or telophase spindle, and image d, the color combined overlay of the two images, depicts dynactin on interpolar microtubules and on the cortex.

a.

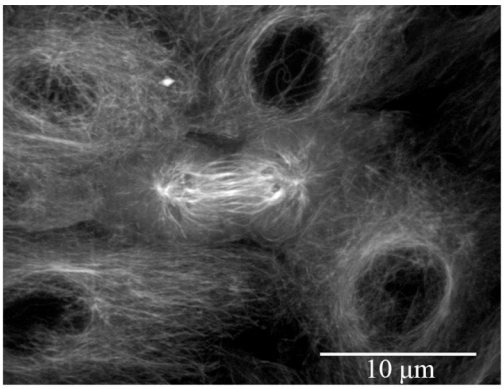

b.

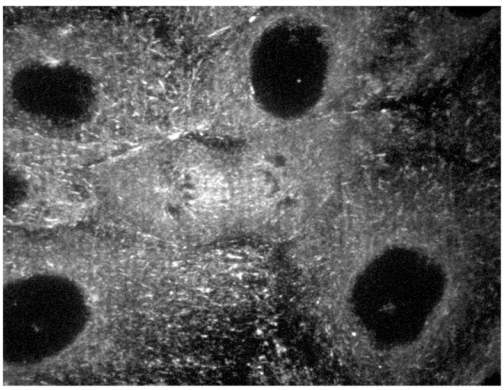

c.

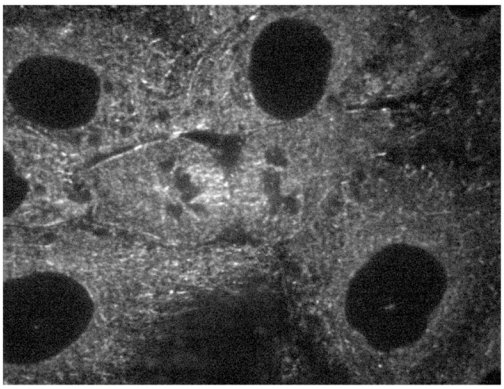

d.

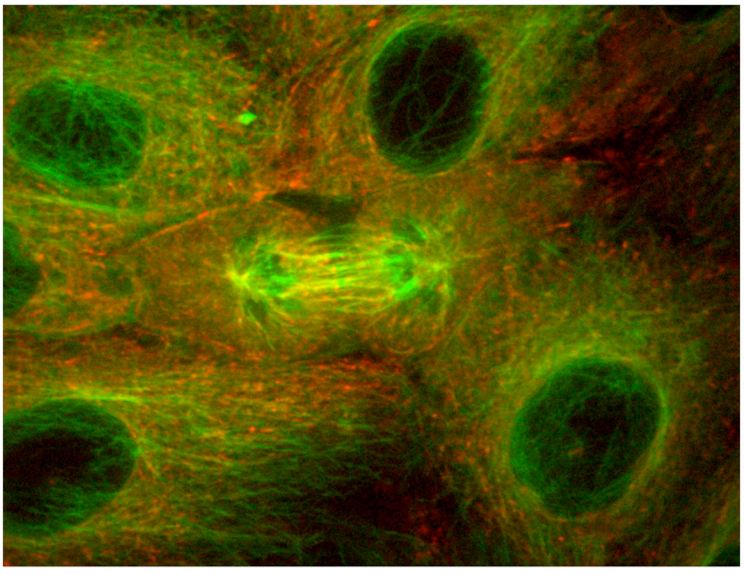

Figure 16. Dynactin Localization in a LLC-Pk1α Cell in Telophase

The maximum projection of fluorescent microtubules in a fixed and stained LLC-Pk1α cell undergoing cytokinesis in telophase is shown in image a. The maximum projection of p150 staining in image b shows dynactin on the tips of microtubules in both the dividing and interphase cells. The color combined overlay of the two images in image c shows little to no dynactin localized to the spindle.

a.

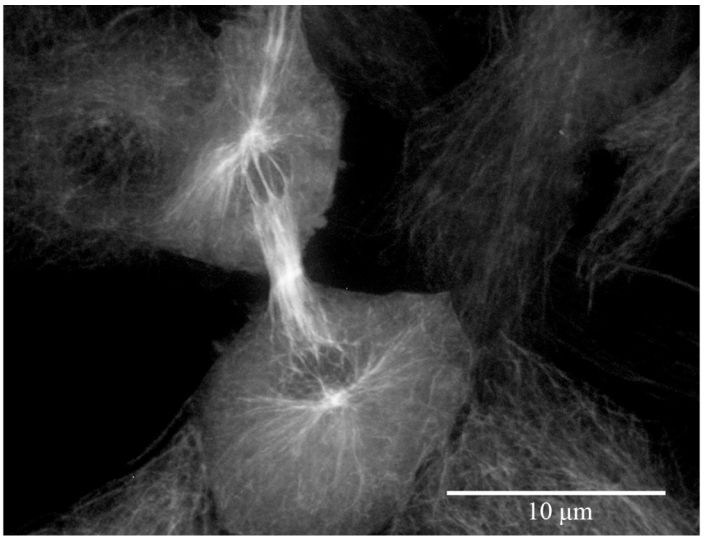

b.

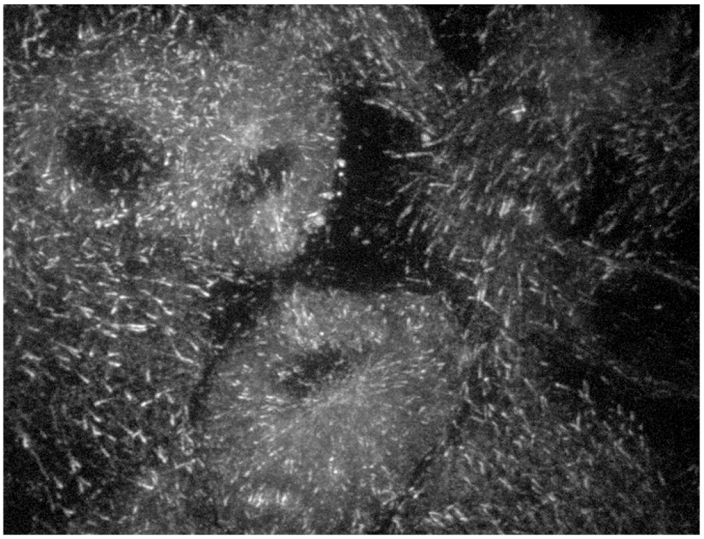

c.

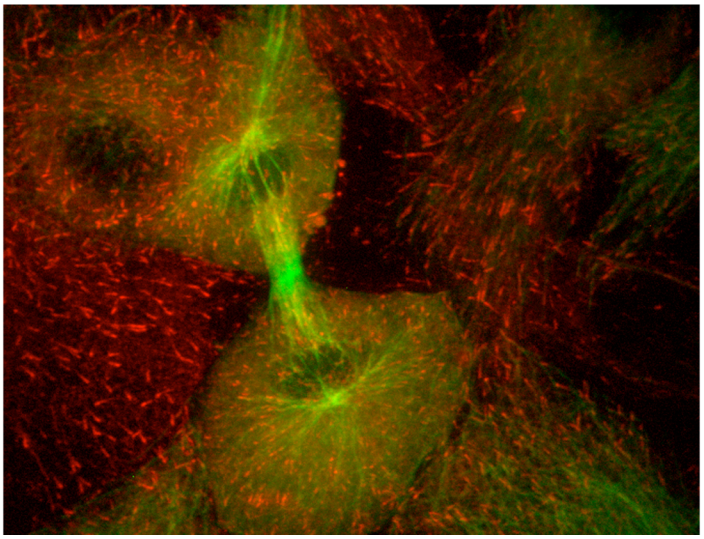

Figure 17. Scoring Fixed LLC-Pk1α Cells Stained for Dynein/Dynactin

The results of scoring of 217 LLC-Pkα cells fixed and stained for p150 are tabulated in this graph by Liz Collins. Cells were scored for dynactin at the cortex, and categorized as either having dynactin at one end (at either end of the long axis of the cell), both ends, one side (the cortex not at either end of the long axis), both sides, or absent from the cortex.

LITERATURE CITED

Ahringer J. 2003. Control of cell polarity and mitotic spindle positioning in animal cells. Curr. Opin. Cell Biol. 15:73-81.

Alberts B. 2008. Molecular biology of the cell. Reference edition. Garland Science, New York.

Altman P. L., and D. D. Katz. 1962. Growth including reproduction and morphological development. Federation of American Societies for Experimental Biology, Washington.

Busson S., D. Dujardin, A. Moreau, J. Dompierre, and J. R. De Mey. 1998. Dynein and dynactin are localized to astral microtubules and at cortical sites in mitotic epithelial cells. Curr. Biol. 8:541-544.

Cairns J. 1975. Mutation selection and the natural history of cancer. Nature 255:197-200.

Carminati J. L., and T. Stearns. 1997. Microtubules orient the mitotic spindle in yeast through dynein-dependent interactions with the cell cortex. J. Cell Biol. 138:629-641.

Chakravarty A., L. Howard, and D. A. Compton. 2004. A mechanistic model for the organization of microtubule asters by motor and non-motor proteins in a mammalian mitotic extract. Mol. Biol. Cell 15:2116-2132.

Couwenbergs C., J. C. Labbe, M. Goulding, T. Marty, B. Bowerman, and M. Gotta. 2007. Heterotrimeric G protein signaling functions with dynein to promote spindle positioning in C. elegans. J. Cell Biol. 179:15-22.

Evan G. I., and K. H. Vousden. 2001. Proliferation, cell cycle and apoptosis in cancer. Nature 411:342-348.

Folsch H., M. Pypaert, S. Maday, L. Pelletier, and I. Mellman. 2003. The AP-1A and AP-1B clathrin adaptor complexes define biochemically and functionally distinct membrane domains. J. Cell Biol. 163:351-362.

Gaetz J., and T. M. Kapoor. 2004. Dynein/dynactin regulate metaphase spindle length by targeting depolymerizing activities to spindle poles. J. Cell Biol. 166:465-471.

Gennerich A., and R. D. Vale. 2009. Walking the walk: how kinesin and dynein coordinate their steps. Curr. Opin. Cell Biol. 21:59-67.

Gibbons I. R., and A. J. Rowe. 1965. Dynein: A Protein with Adenosine Triphosphatase Activity from Cilia. Science 149:424-426.

Grill S. W., and A. A. Hyman. 2005. Spindle positioning by cortical pulling forces. Dev. Cell. 8:461-465.

Hara Y., and A. Kimura. 2009. Cell-size-dependent spindle elongation in the Caenorhabditis elegans early embryo. Curr. Biol. 19:1549-1554.

Hull R. N., W. R. Cherry, and G. W. Weaver. 1976. The origin and characteristics of a pig kidney cell strain, LLC-PK. In. Vitro. 12:670-677.

Karki S., and E. L. Holzbaur. 1999. Cytoplasmic dynein and dynactin in cell division and intracellular transport. Curr. Opin. Cell Biol. 11:45-53.

King S. M. 2000. AAA domains and organization of the dynein motor unit. J. Cell. Sci. 113 (Pt 14):2521-2526.

Kittler R., L. Pelletier, C. Ma, I. Poser, S. Fischer, A. A. Hyman, and F. Buchholz. 2005. RNA interference rescue by bacterial artificial chromosome transgenesis in mammalian tissue culture cells. Proc. Natl. Acad. Sci. U. S. A. 102:2396-2401.

Kozlowski C., M. Srayko, and F. Nedelec. 2007. Cortical microtubule contacts position the spindle in C. elegans embryos. Cell 129:499-510.

Labbe J. C., P. S. Maddox, E. D. Salmon, and B. Goldstein. 2003. PAR proteins regulate microtubule dynamics at the cell cortex in C. elegans. Curr. Biol. 13:707-714.

Markus S. M., J. J. Punch, and W. L. Lee. 2009. Motor- and tail-dependent targeting of dynein to microtubule plus ends and the cell cortex. Curr. Biol. 19:196-205.

McCarthy E. K., and B. Goldstein. 2006. Asymmetric spindle positioning. Curr. Opin. Cell Biol. 18:79-85.

Mizuno N., A. Narita, T. Kon, K. Sutoh, and M. Kikkawa. 2007. Three-dimensional structure of cytoplasmic dynein bound to microtubules. Proc. Natl. Acad. Sci. U. S. A. 104:20832-20837.

Muyrers J. P., Y. Zhang, V. Benes, G. Testa, J. M. Rientjes, and A. F. Stewart. 2004. ET recombination: DNA engineering using homologous recombination in E. coli. Methods Mol. Biol. 256:107-121.

Myers K. R., K. W. Lo, R. J. Lye, J. M. Kogoy, V. Soura, M. Hafezparast, and K. K. Pfister. 2007. Intermediate chain subunit as a probe for cytoplasmic dynein function: biochemical analyses and live cell imaging in PC12 cells. J. Neurosci. Res. 85:2640-2647.

Nielsen R., H. Birn, S. K. Moestrup, M. Nielsen, P. Verroust, and E. I. Christensen. 1998. Characterization of a kidney proximal tubule cell line, LLC-PK1, expressing endocytotic active megalin. J. Am. Soc. Nephrol. 9:1767-1776.

O'Connell C. B., and Y. L. Wang. 2000. Mammalian spindle orientation and position respond to changes in cell shape in a dynein-dependent fashion. Mol. Biol. Cell 11:1765-1774.

Oiwa K., and H. Sakakibara. 2005. Recent progress in dynein structure and mechanism. Curr. Opin. Cell Biol. 17:98-103.

Pecreaux J., J. C. Roper, K. Kruse, F. Julicher, A. A. Hyman, S. W. Grill, and J. Howard. 2006. Spindle oscillations during asymmetric cell division require a threshold number of active cortical force generators. Curr. Biol. 16:2111-2122.

Pfarr C. M., M. Coue, P. M. Grissom, T. S. Hays, M. E. Porter, and J. R. McIntosh. 1990. Cytoplasmic dynein is localized to kinetochores during mitosis. Nature 345:263-265.

Sugimoto H., M. Sugahara, H. Folsch, Y. Koide, F. Nakatsu, N. Tanaka, T. Nishimura, M. Furukawa, C. Mullins, N. Nakamura, I. Mellman, and H. Ohno. 2002. Differential recognition of tyrosine-based basolateral signals by AP-1B subunit mu1B in polarized epithelial cells. Mol. Biol. Cell 13:2374-2382.

Tanenbaum M. E., L. Macurek, N. Galjart, and R. H. Medema. 2008. Dynein, Lis1 and CLIP-170 counteract Eg5-dependent centrosome separation during bipolar spindle assembly. EMBO J. 27:3235-3245.

Tolic-Norrelykke I. M. 2010. Force and length regulation in the microtubule cytoskeleton: lessons from fission yeast. Curr. Opin. Cell Biol. 22:21-28.

Toyoshima F., and E. Nishida. 2007. Integrin-mediated adhesion orients the spindle parallel to the substratum in an EB1- and myosin X-dependent manner. EMBO J. 26:1487-1498.

Tulu U. S., C. Fagerstrom, N. P. Ferenz, and P. Wadsworth. 2006. Molecular requirements for kinetochore-associated microtubule formation in mammalian cells. Curr. Biol. 16:536-541.

Vaughan P. S., J. D. Leszyk, and K. T. Vaughan. 2001. Cytoplasmic dynein intermediate chain phosphorylation regulates binding to dynactin. J. Biol. Chem. 276:26171-26179.

Warming S., N. Costantino, D. L. Court, N. A. Jenkins, and N. G. Copeland. 2005. Simple and highly efficient BAC recombineering using galK selection. Nucleic Acids Res. 33:e36.